

## Modelling the influence of vitamin D and probiotic supplementation on the microbiome and immune response

S.J. FRANKS\*

*School of Mathematical Sciences, University of Nottingham, Nottingham, UK*

J.L. DUNSTER

*School of Mathematical Sciences, University of Nottingham, Nottingham, UK*

*Institute for Cardiovascular and Metabolic Research, University of Reading, Reading, UK*

S.R. CARDING

*Quadram Institute Biosciences, Norwich Research Park, Norwich, UK*

*Norwich Medical School, University East Anglia, Norwich, UK*

J.M. LORD

*Institute of Inflammation and Ageing, University of Birmingham, Birmingham, UK*

M. HEWISON

*Institute of Metabolism and Systems Research, University of Birmingham, Birmingham, UK*

P.C. CALDER

*School of Human Development and Health, Faculty of Medicine, University of Southampton, Southampton, UK*

AND

J.R. KING

*School of Mathematical Sciences, University of Nottingham, Nottingham, UK*

\*Corresponding author: [susan.franks@nottingham.ac.uk](mailto:susan.franks@nottingham.ac.uk)

[Received on Date Month Year; revised on Date Month Year; accepted on Date Month Year]

The intestinal microbiota play a critical role in human health and disease, maintaining metabolic and immune/inflammatory health, synthesising essential vitamins and amino acids and maintaining intestinal barrier integrity. The aim of this paper is to develop a mathematical model to describe the complex interactions between the microbiota, vitamin D/vitamin D receptor (VDR) pathway, epithelial barrier and immune response in order to understand better the effects of supplementation with probiotics and vitamin D. This is motivated by emerging data indicating the beneficial effects of vitamin D and probiotics individually and when combined. We propose a system of ordinary differential equations determining the time evolution of intestinal bacterial populations, concentration of the VDR:1,25(OH)<sub>2</sub>D complex in epithelial and immune cells, the epithelial barrier and the immune response. The model shows that administration of probiotics and/or vitamin D upregulates the VDR complex, which enhances barrier function and protects against intestinal inflammation. The model also suggests co-supplementation to be superior to individual supplements. We explore the effects of inflammation on the populations of commensal and pathogenic bacteria and the vitamin D/VDR pathway and discuss the value of gathering additional experimental data motivated by the modelling insights.

**Keywords:** Microbiota; Vitamin D Receptor; Inflammation and immune response; Supplementation.

## 1. Introduction

Understanding the complex interactions between the intestinal microbiota, vitamin synthesis, intestinal barrier integrity and the immune response, including its inflammatory component, is crucial for better comprehension of human health and disease (Abboud et al. 2020). Dysbiosis (i.e. an imbalance in microbial composition, changes in microbial metabolism, or changes in microbial distribution throughout the gastrointestinal tract) or adverse changes to the intestinal microbiota composition due to lifestyle and behavioural factors (e.g. medications and antibiotics, adopting a poor diet or changes in geography), damage to the host-microbiota interface, or alterations of the immune system can result in an increased susceptibility to pathogenic invasion and the onset of infectious disease. Such dysregulation can also result in a heightened immune response and chronic inflammation resulting in tissue damage and various diseases e.g. inflammatory bowel disease (IBD), obesity and diabetes (Cristofori et al. 2021).

Manipulation of the intestinal microbiota with dietary components such as prebiotics, probiotics and vitamin D has been shown to contribute to the restoration of normobiosis (Tangestani et al. 2021). Increased vitamin D receptor (VDR) expression by epithelial and immune cells may decrease microbial dysbiosis, enhance barrier function, increase the expression of antimicrobial peptides (AMPs), decrease pro-inflammatory cytokines and increase the production of beneficial short-chain fatty acids (SCFAs) (Abboud et al. 2020, Tangestani et al. 2021, Xong et al. 2020). AMPs (mainly defensins and cathelicidins) are key regulators of interactions between constituents of the microbiota and host tissues and exert a range of antimicrobial activities via sequestering key growth nutrients, permeabilising bacterial membranes and other related mechanisms, thereby playing an important role in the maintenance of both microbial homeostasis and host defence (Xong et al. 2020). Vitamin D has also been shown to preserve intestinal barrier homeostasis and tight junction complexes in the intestinal epithelium reducing dysbiosis and bacterial colonisation (Tangestani et al. 2021).

Likewise, probiotics, which are ingestible health promoting living microorganisms, have also been shown to improve the balance of the intestinal microbiota by regulating its constituents and metabolic output (de Vos et al. 2017). Probiotics have been associated with protective effects in the intestine, with some strains regulating immune cells via the interaction of bacterial cell-wall components or secreted bacterial products with immune or epithelial cells in the intestinal mucosa (de Vos et al. 2017). Others induce alterations in production of pro-inflammatory and regulatory cytokines (Stojanov et al. 2020) or beneficially contribute to the organisation of the epithelial tight junctions via regulation of specific tight junction proteins (e.g. occludin) (de Vos et al. 2017, Mujagic et al. 2017).

The beneficial effects of combined supplementation with vitamin D and probiotics in modulating the intestinal microbiota, in addition to fostering healthy microbe–host interactions, are discussed in (Abboud et al. 2020, Pagnini et al. 2021). This co-supplementation provides a possible therapeutic option for diseases such as IBD. Probiotics have been shown to increase intestinal vitamin D absorption, and to increase VDR protein expression and transcriptional activity (Singh et al. 2020). Likewise, VDR status seems to regulate the mechanisms of action of probiotics and modulate their anti-inflammatory, immunomodulatory and anti-infective benefits, suggesting a bidirectional interaction (Pagnini et al. 2021, Bishop et al. 2020).

While models describing the microbiome (Magnúsdóttir et al. 2018, Kumar et al. 2019, Shashkova et al. 2016, Adrian 2020), vitamin D metabolism (Chun et al. 2012, Beetjes et al. 2019), the immune system in response to pathogens (Stübler et al. 2023) and coupled microbe-immune system interaction (Hara et al. 2019) are available in the literature, the aim of this paper is to develop a novel mathematical model to describe for the first time the complex interactions between the microbiota, the intestinal barrier, vitamin D and the immune response in order to understand better the effects of individual

47 and co-supplementation of vitamin D and probiotics. The model seeks to be at a level of complexity  
 48 appropriate to the nature of the biological components and available data.

49 The complete model is split into three sub-models. These are described, along with their parameter  
 50 values for the intestinal nutrients and bacteria (Subsection 2.1), vitamin D and its metabolites  
 51 (Subsection 2.2) and the epithelial barrier and immune response (Subsection 2.3), along with  
 52 simulations with and without inflammation. We believe these individual models to be of interest  
 53 in their own right and are combined in Section 3 and solved numerically to assess the impact of  
 54 vitamin D supplements only (Subsection 3.2), probiotics only (Subsection 3.3) and co-supplementation  
 55 (Subsection 3.4).

56 The full model will enable investigation into the proposed beneficial effects observed experimentally  
 57 of combined supplementation, with the goal of determining whether they might improve human health.

## 58 2. Model Formulation

59 The schematic shown in Figure 1 summarises the complex interactions between the three submodels  
 i.e. the intestinal microbiota, vitamin D and the immune response captured by the model. We begin

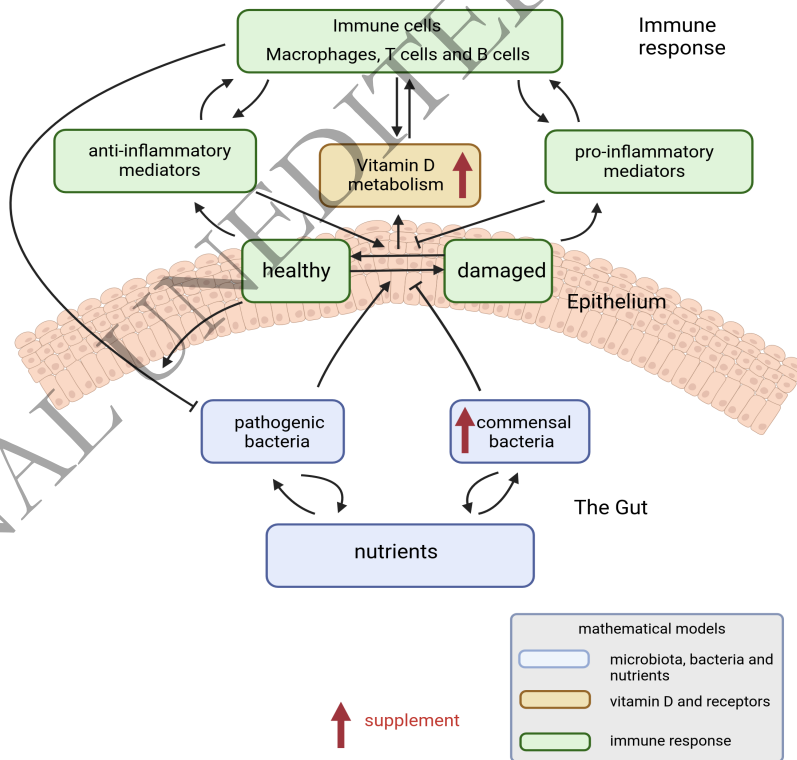


FIG. 1. The interactions between the microbiota, vitamin D and the immune response captured in the mathematical models presented in Sections 2.1, 2.2 and 2.3, respectively.

by providing a detailed derivation and explanation of the mathematical equations for each of these processes individually. Baseline parameters and the sensitivity of the model to these are discussed for each sub-model and simulations presented to verify behaviour. We then consider the full model, combining the three model components, to predict the effect of vitamin D and probiotic interventions on the system. The code, in the form of a R notebook, for these latter simulations is provided in the supplementary material. ODEs were solved using the ode solver in R with the default integrator lsoda.

A summary of each dependent variable in the model, along with its units, is given in Table 1.

Variable	Description	Units	Variable	Description	Units
$N_{ma}$	Concentration of macronutrients	ng/ml	$N_{mi}$	Concentration of micronutrients	ng/ml
$N_{mb}$	Concentration of metabolites	ng/ml	$N_a$	Concentration of alternate nutrients	ng/ml
$F$	Population of commensal bacteria	CFU	$P$	Population of pathogenic bacteria	CFU
$D$	Extracellular concentration of 25(OH)D	ng/ml	$D_a$	Extracellular concentration of 1,25(OH) <sub>2</sub> D	ng/ml
$D_i$	Intracellular concentration of 25(OH)D	ng/ml	$D_{a_i}$	Intracellular concentration of 1,25(OH) <sub>2</sub> D	ng/ml
$V_{D_a}$	Concentration of VDR:1,25(OH) <sub>2</sub> D complex	ng/ml	$E$	Volume fraction of healthy epithelial cells	no units
$E_d$	Volume fraction of damaged epithelial cells	no units	$M$	Density of macrophages	cells/ml
$T_h$	Density of T-helper cells	cells/ml	$R$	Density of regulatory cells	cells/ml
$G$	Concentration of anti-inflammatory cytokines	ng/ml	$B$	Density of plasma B cells	cells/ml
$t$	Time	days	$C$	Concentration of pro-inflammatory cytokines	ng/ml

TABLE 1 Description and units of the dependent variables in the full model.

66

### 2.1. The microbiota

The microbiota consists of several groups of microorganisms, including bacteria, archaea, yeast, and viruses. In our model we simplify to include two populations of bacteria, namely commensals  $F$  (of which over 90% are represented by the two phyla Firmicutes and Bacteroidetes) and pathogenic bacteria  $P$  (such as *Salmonella* and invasive *E. coli*).

Interactions between bacteria, nutrients and epithelial cells are described in (Fan et al. 2021, Pickard et al. 2017 and Zhou et al. 2022) and summarised as follows: macronutrients  $N_{ma}$  (e.g. carbohydrates, protein, fat, fibre) and micronutrients  $N_{mi}$  (e.g. vitamins and minerals) are consumed from the diet at rates  $N_{ma}^0$  and  $N_{mi}^0$ , respectively, with intestinal microbes and epithelial cells competing for the latter at rates  $\eta_3$  (commensals),  $\eta_4$  (pathogens) and  $\eta_5$  (epithelial cells). Commensal bacteria principally convert macronutrients by fermentation into metabolites  $N_{mb}$  (e.g. SCFAs) at rate  $\eta_1$ , most of these metabolites being absorbed by the intestinal mucosa, both providing important fuel for the proliferation of intestinal epithelial cells (rate  $\eta_6$ ) and having beneficial effects on immune cells through induction of intracellular or extracellular processes. Metabolites support epithelial barrier integrity and function through induction of genes encoding tight junction components and exert anti-inflammatory effects in the intestinal mucosa by inducing anti-inflammatory cytokines. Gases (e.g. hydrogen and methane) are also produced during fermentation which can be utilised by some commensal microbes at rate  $\eta_7$  whilst other gases need to be expelled (e.g. hydrogen sulphide). Pathogens induce intestinal inflammation and use virulence factors or toxins to enable conversion of metabolic byproducts generated by commensal

85

86 bacteria into alternate nutrients  $N_a$  (e.g. carbohydrates, ethanolamine) at rate  $\eta_8$ . Some toxins (e.g.  
 87 Shiga toxin) can also directly rupture the epithelial barrier, but we do not consider this mechanism  
 88 here. The alternate nutrients are utilised as an energy source by pathogenic bacteria at rate  $\eta_9$ , giving  
 89 them an advantage over commensals as they lack this ability. If pathogenic bacteria bypass or avoid  
 90 microbiota-based defences to reach host cells, they can be taken up by the cells via endocytic pathways  
 91 and degraded by phagolysosomes, releasing micronutrients from the breakdown of the cell components  
 92 at rate  $\eta_2$ . Autophagy plays a role in this mechanism and is regulated by the gene ATG16L1 and can  
 93 be induced by SCFAs (Bakke et al. 2018). We assume that excess macronutrients, micronutrients,  
 94 metabolites and alternate nutrients are removed from the gastrointestinal tract in the faeces or flatulence  
 at the same rate  $q$ . A summary of these interactions is shown in Figure 2.

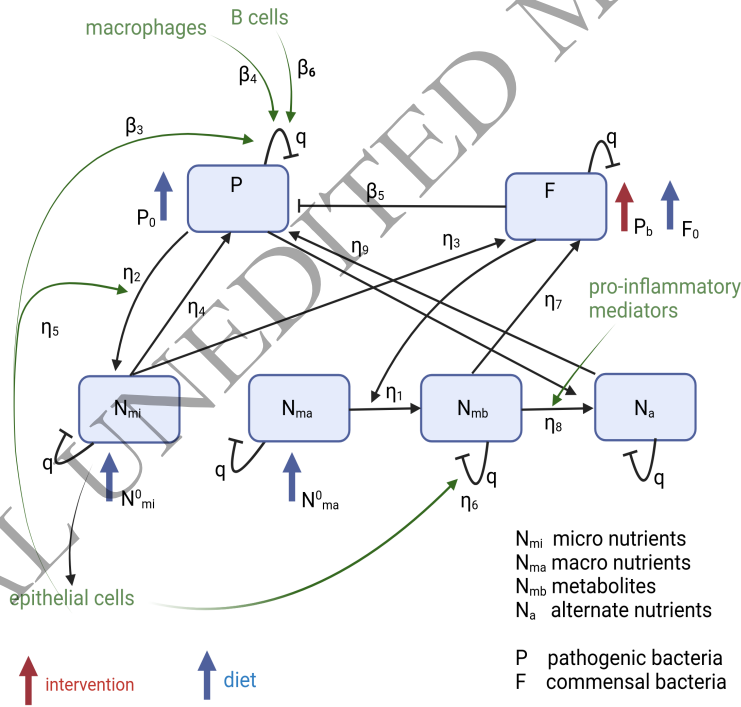


FIG. 2. **The microbiota and nutrient network.** The model derived in equations (2.1)-(2.6) captures the reactions between commensal and pathogenic bacteria, macronutrients, micronutrients, metabolites and alternate nutrients. The rates are defined in Table 2.

96 The equations governing the concentrations of the different nutrient types are then

$$\frac{dN_{ma}}{dt} = N_{ma}^0 - \eta_1 FN_{ma} - qN_{ma}, \quad (2.1)$$

$$\frac{dN_{mi}}{dt} = N_{mi}^0 + \eta_2 N_{mb} EP - \eta_3 FN_{mi} - \eta_4 PN_{mi} - \eta_5 EN_{mi} - qN_{mi}, \quad (2.2)$$

$$\frac{dN_{mb}}{dt} = \eta_1 FN_{ma} - \eta_6 EN_{mb} - \eta_7 FN_{mb} - \eta_8 N_{mb} CP - qN_{mb}, \quad (2.3)$$

$$\frac{dN_a}{dt} = \eta_8 N_{mb} CP - \eta_9 N_a P - qN_a, \quad (2.4)$$

97 where  $E$  represents the volume fraction of epithelial cells that are healthy, with tight junctions between  
 98 them (so that  $E = 1 - E_d$  where  $E_d$  is the volume fraction of damaged epithelial cells) and  $C$  denotes the  
 99 concentration of pro-inflammatory mediators which we assume to be a measure of inflammation. We  
 100 assume in this sub-model that they are both constant. Over 90% of SCFAs produced by the intestinal  
 101 microbiota are absorbed by the mucosa to support the growth and proliferation of epithelial cells  
 102 (Conlon et al. 2014) so we assume that  $\eta_6 E \gg \eta_7 F$  and  $\eta_8 CP$ .

103 We assume that commensal and pathogenic bacteria acquired from diet and the environment  
 104 enter the intestinal tract at rates  $F^0$  and  $P^0$ , respectively. We include an additional input term for  
 105 the commensal bacteria population to incorporate probiotic supplementation at rate  $P_b$ . Probiotics  
 106 are identified by specific strains (e.g. *Lactobacillus*, *Bifidobacterium*) that influence the intestinal  
 107 microbiota in different ways. Here we assume that they increase the number of commensals,  
 108 which will enhance the production of beneficial bioactive metabolites. We assume that commensal  
 109 bacteria proliferation depends upon availability of micronutrients and metabolites (converted from  
 110 macronutrients) and the rates of proliferation are proportional to the consumption rates  $\eta_3$  and  
 111  $\eta_7$ , respectively, with proportionality constant  $\beta_1$ . The pathogenic bacteria also compete for the  
 112 micronutrients and utilise these and the alternate nutrients (converted from metabolites) for proliferation  
 113 at rates proportional to their rates of consumption  $\eta_4$  and  $\eta_9$ , respectively, with proportionality constant  
 114  $\beta_2$ .

115 In addition, commensal microbes mediate pathogen colonization resistance by producing toxic/  
 116 anti-microbial substances e.g. bacteriocins, secondary bile acids and fermentation products such as  
 117 SCFAs and AMPs that directly inhibit the growth of pathogens at rate  $\beta_5$ . Commensals also enhance  
 118 intestinal barrier function via their impact on tight junction proteins and mucus production and induce  
 119 AMP production by epithelial cells and autophagy to destroy pathogens at rate  $\beta_3$ . They also activate  
 120 the immune response by stimulating innate phagocytic cells (e.g. macrophages) to produce AMPs and  
 121 recruit other innate and adaptive immune cells to contain and eradicate pathogens at rate  $\beta_4$ . Activated  
 122 mucosal plasma B cells produce antibodies, specifically immunoglobulin A (IgA), which is transported  
 123 by intestinal epithelial cells into the mucus layer where it becomes secretory IgA (sIgA). sIgA coats  
 124 pathogens, directly hindering their function and facilitates recognition and subsequent elimination of  
 125 pathogens by innate immune cells at rate  $\beta_6$ . Note that we do not include adhesion or niche exclusion in  
 126 our model. Commensal and pathogenic bacteria are removed from the system by degradation or flushed  
 127 out in the faeces and we assume this happens at the same rate as the excess nutrient removal i.e.  $q$ .



The equations governing the number of bacteria in the two populations are then given by

$$\frac{dF}{dt} = F^0 + P_b + f(B_T)\beta_1(\eta_3N_{mi} + \eta_7N_{mb})F - qF, \quad (2.5)$$

$$\frac{dP}{dt} = P^0 + f(B_T)\beta_2(\eta_4N_{mi} + \eta_9N_a)P - \beta_3EP - \beta_4MP - \beta_5FP - \beta_6BP - qP, \quad (2.6)$$

where  $M$  denotes the density of macrophages,  $B$  the density of activated plasma B cells (both assumed constant in this sub-model) and the dimensionless growth function  $f(B_T)$ , defined by

$$f(B_T) = 1 - \frac{B_T}{K}$$

represents logistic growth with carrying capacity  $K$  so that the growth of the total population density of bacteria  $B_T = F + P$  has a maximum size  $K$  which can be sustained in the intestine given the resources available.

We assume the microbiota are in homeostasis and consist mainly of commensal bacteria at  $t = 0$ , i.e.

$$N_{ma0} = N_{ma_{ss}}, \quad N_{mi0} = N_{mi_{ss}}, \quad N_{mb0} = N_{mb_{ss}}, \quad N_{a0} = N_{a_{ss}}, \quad F_0 = 0.99 \times 10^{14}, \quad P_0 = 0.01 \times 10^{14}, \quad (2.7)$$

where subscript  $_{ss}$  denotes the nutrient concentration at steady state.

### 2.1.1. Parameter values and sensitivity analysis for microbiome model

Parameter values are not readily available. However, we can make estimates for the consumption rate of macronutrients  $N_{ma}^0$ , micronutrients  $N_{mi}^0$ , commensal  $F^0$  and pathogenic bacteria  $P^0$ , the rate of removal of these in the faeces  $q$  and also the carrying capacity  $K$  (see Table 2). Note that we do not take into account the gastrointestinal transit times. From clinical studies we also know approximate rates of intake of probiotics  $P_b$ . The number of microbes consumed in the diet is given in Lang et al. 2014 as  $1.3 \times 10^9$  CFU/day and we assume that pathogenic bacteria make up approximately 5% of the total intake. We also assume that the daily intake of macronutrients and micronutrients, the rate of removal of nutrients and bacteria in the faeces and the daily intake of commensal and pathogenic bacteria are all proportional. These are summarised, along with estimates for the remaining parameters not available in the literature, in Table 2. These have been chosen to produce biologically realistic results.

Given the considerable uncertainty in the choice of parameter values, a standard local sensitivity analysis is performed to analyse the effects of changing the individual parameters on the nutrient concentrations and bacterial populations. The following method is also applied to the vitamin D and vitamin D receptor, epithelial barrier and immune response models described in Sections 2.2.1 and 2.3.1.

*Method for sensitivity analysis.* Using the baseline parameter values in Table 2, we solve our system of ODEs (2.1)-(2.6) to large time to determine the nutrient concentrations and bacterial populations at steady state. We then estimate the local effect of parameters on these steady states by increasing and decreasing each parameter individually by 10%, and again, solving to large time to determine the new steady state. The sensitivity is then calculated by the relative change in our output variable at steady

Parameter	Description	Value	Units
$N_{ma}^0$	Rate of intake of macronutrients	400	g/day
$N_{mi}^0$	Rate of intake of micronutrients	9	g/day
$q$	Rate of faecal removal of excess nutrients and bacteria	0.13	day <sup>-1</sup>
$F^0$	Rate of intake of commensal bacteria	$1.24 \times 10^9$	CFU/day
$P^0$	Rate of intake of pathogenic bacteria	$0.06 \times 10^9$	CFU/day
$P_b$	Rate of intake of probiotics	$1 \times 10^9 - 1 \times 10^{11}$	CFU/day
$K$	Carrying capacity	$1 \times 10^{14}$	CFU
$\eta_1$	Rate of uptake of macronutrients by commensal bacteria	$1 \times 10^{-14}$	(CFU.day) <sup>-1</sup>
$\eta_2$	Rate of release of micronutrients from degradation of pathogenic bacteria	$1 \times 10^{-17}$	(CFU.day) <sup>-1</sup>
$\eta_3$	Rate of consumption of micronutrients by commensal bacteria	$1 \times 10^{-14}$	(CFU.day) <sup>-1</sup>
$\eta_4$	Rate of uptake of micronutrients by pathogenic bacteria	$1 \times 10^{-14}$	(CFU.day) <sup>-1</sup>
$\eta_5$	Rate of consumption of micronutrients by host epithelial cells	0.01	day <sup>-1</sup>
$\eta_6$	Rate of utilisation of metabolites by epithelial cells	0.1	day <sup>-1</sup>
$\eta_7$	Rate of utilisation of metabolites by commensal bacteria	$1 \times 10^{-17}$	(CFU.day) <sup>-1</sup>
$\eta_8$	Rate of production of alternate nutrients	$1.3 \times 10^{-9}$	ml/(ng.CFU.day)
$\eta_9$	Rate of consumption of alternate nutrients by pathogens	$1 \times 10^{-14}$	(CFU.day) <sup>-1</sup>
$\beta_1$	Proportionality parameter	$2.44 \times 10^5$	CFU/ng
$\beta_2$	Proportionality parameter	$2.44 \times 10^4$	CFU/ng
$\beta_3$	Rate at which pathogenic bacteria are destroyed by autophagy and AMPs from epithelial cells	0.5	day <sup>-1</sup>
$\beta_4$	Rate at which pathogens are destroyed by macrophages	$9.17 \times 10^{-9}$	ml/day
$\beta_5$	Rate at which pathogens are destroyed by commensals	$1 \times 10^{-17}$	(CFU.day) <sup>-1</sup>
$\beta_6$	Rate at which pathogens are destroyed by sIgA	$1.03 \times 10^{-6}$	ml/day

TABLE 2 Definition, value and units of the nutrient model parameters. In developed countries, adults consume on average approximately 400 g/day of macronutrients and 9 g/day of micronutrients (Salazar et al. 2019). They typically expel 128 g/day of faeces of which there are approximately  $1 \times 10^{11}$  bacteria/g of wet stool so that the total number of bacteria removed in the faeces is  $1.28 \times 10^{13}$  bacteria/day<sup>-1</sup> (Sender et al. 2016). Expressing this in terms of the total number of bacteria in the intestine gives an approximate value of  $q = 0.13$  day<sup>-1</sup>. In a healthy diet we consume approximately  $1.3 \times 10^9$  CFU/day (Lang et al. 2014) and we assume 5% of these microbes are pathogenic. There are approximately  $1 \times 10^{14}$  CFU of bacteria in the intestinal tract so we assume that the carrying capacity  $K$  equals this value.

158 state in relation to the relative change in the parameter i.e.

$$\text{Sensitivity} = \frac{\Delta y / y}{|\Delta \theta| / \theta} \quad (2.8)$$

159 where  $y$  is the output variable, i.e.  $N_{ma}$ ,  $N_{mi}$ ,  $N_{mb}$ ,  $N_a$ ,  $F$  and  $P$ , and  $\theta$  is the parameter so that  $\Delta \theta =$   
 160  $1.1 \times \theta$  and  $\Delta \theta = 0.9 \times \theta$ . This provides a measure of how much the concentration of nutrients or  
 161 number of bacteria increase or decrease in relation to an up- or down-regulation in the parameter value.



162 We assume that values for the volume fraction of healthy epithelial cells  $E$ , macrophage density  $M$ ,  
 163 pro-inflammatory cytokine concentration  $C$  and plasma B cell density  $B$  are constant i.e.

$$E = 0.9, \quad C = 0.45 \text{ pg/ml}, \quad M = 4.9 \times 10^5 \text{ cells/ml}, \quad B = 3.8 \times 10^3 \text{ cells/ml},$$

164 representing low levels of inflammation in which the epithelial barrier is compromised, increasing  
 165 signalling of pro-inflammatory cytokines that activate macrophages and B cells. Concentrations and  
 166 densities have been approximated to be half the measured values from in-house human data on the  
 167 pro-inflammatory cytokine IFN- $\gamma$ , plasma B cells and macrophages in blood in diseased individuals  
 168 experiencing inflammation.

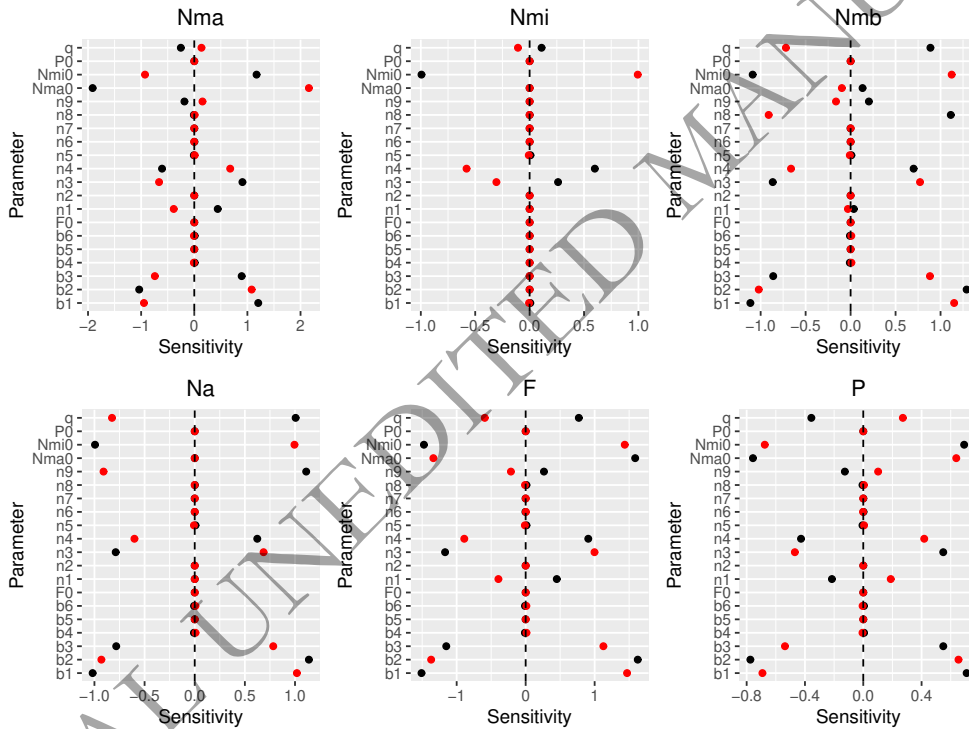


FIG. 3. The effect of varying parameter values on the steady state concentrations of macronutrients, micronutrients, metabolites and alternate nutrients and the number of commensal and pathogenic bacteria. Baseline parameter values are taken from Table 2 and each parameter is sequentially varied by a 10% decrease (black) and a 10% increase (red). Sensitivity is defined by equation (2.8). We assume low levels of inflammation so  $E = 0.9$ ,  $C = 0.45 \text{ pg/ml}$ ,  $M = 4.9 \times 10^5 \text{ cells/ml}$ ,  $B = 3.8 \times 10^3 \text{ cells/ml}$ . Note that  $n=\eta$  and  $b=\beta$ .

169 Figure 3 demonstrates that the parameters that are the most influential on the bacterial populations  
 170 are the rates of intake of micronutrients  $N_{mi}^0$  and macronutrients  $N_{ma}^0$ , proportionality parameters  $\beta_1$   
 171 and  $\beta_2$ , the rate at which pathogenic bacteria are destroyed by autophagy and AMPs from epithelial  
 172 cells  $\beta_3$ , the consumption of micronutrients by commensals  $\eta_3$  and the rate of uptake of micronutrients  
 173 by pathogenic bacteria  $\eta_4$  and the rate of faecal removal  $q$ . A decrease in  $q$ , the rate of production  
 174 of alternate nutrients  $\eta_8$ ,  $\eta_4$  and  $\beta_2$  and an increase in  $N_{mi}^0$ ,  $\eta_3$ ,  $\beta_3$  and  $\beta_1$  results in an increase

175 in metabolites, which are utilised by the commensal bacteria resulting in growth of the commensal  
 176 population and a decline in pathogens. A decrease in  $N_{mi}^0$ ,  $\eta_3$ ,  $\beta_1$ ,  $\beta_3$ , the rate of consumption of  
 177 macronutrients by commensals  $\eta_1$  and an increase in  $N_{ma}^0$ ,  $\beta_2$  and  $\eta_4$  increases the concentration of  
 178 macronutrients, which decreases the concentration of metabolites, inhibiting the commensal population.  
 179 Similarly, a decrease in  $\eta_3$  and  $\eta_4$  and an increase in  $N_{mi}^0$  increases the concentration of micronutrients  
 180 that are consumed by the pathogens, also inhibiting the commensal population.

181 The sensitivity of the model to the immune/inflammatory variables, i.e.  $E$ ,  $C$ ,  $M$ ,  $B$ , is shown  
 182 in Figure 4 keeping the baseline parameters in Table 2 constant and increasing and decreasing the  
 183 values for  $E$ ,  $C$ ,  $M$  and  $B$  above by 10%. All of the variables are sensitive to changes in the  
 184 volume fraction of healthy epithelial cells, in particular, macronutrients, micronutrients and pathogens  
 185 decline with an increase in  $E$  whilst metabolites, alternate nutrients and commensals increase. The  
 186 concentration of metabolites is also influenced by the concentration of pro-inflammatory cytokines.  
 187 The densities of macrophages and plasma B cells are not influential on the bacterial populations or  
 188 nutrient concentrations for the specified changes of magnitude.

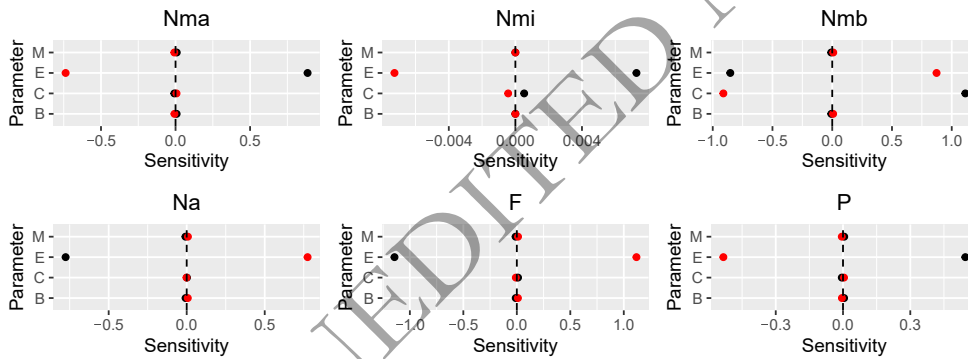


FIG. 4. The effect of varying parameter values on the steady state concentrations of macronutrients, micronutrients, metabolites and alternate nutrients and the number of commensal and pathogenic bacteria. Baseline parameter values are taken from Table 2 with  $E$ ,  $B$ ,  $C$  and  $M$  sequentially varied by a 10% decrease (black) and a 10% increase (red). Sensitivity is defined by equation (2.8).

189 As the system of equations is too complicated to solve analytically for the steady state solutions, we  
 190 also consider sensitivity of the model to a wide range of initial data to large time and Figure 5 illustrates  
 191 how the steady state values of the model variables change with an increasing initial pathogen population  
 192  $P_0$  with the initial concentrations of nutrients and population of commensal bacteria remaining constant.  
 193 When the initial pathogen population exceeds a certain threshold (approximately  $>1 \times 10^{12}$  CFU), the  
 194 pathogenic bacteria dominate, utilising the alternate nutrients to proliferate faster than the rate they are  
 195 being destroyed by AMPs and the inflammatory response. This indicates that the system is bistable,  
 196 suggesting that when the microbiome is in sufficient dysbiosis, it triggers the transition from a non-  
 197 inflammatory to an inflammatory steady state.

198 Changes in initial nutrient concentrations and the population of commensals (not shown) do not  
 199 influence the steady state values of  $N_{ma}$ ,  $N_{mi}$ ,  $N_{mb}$ ,  $N_a$ ,  $F$  and  $P$ .

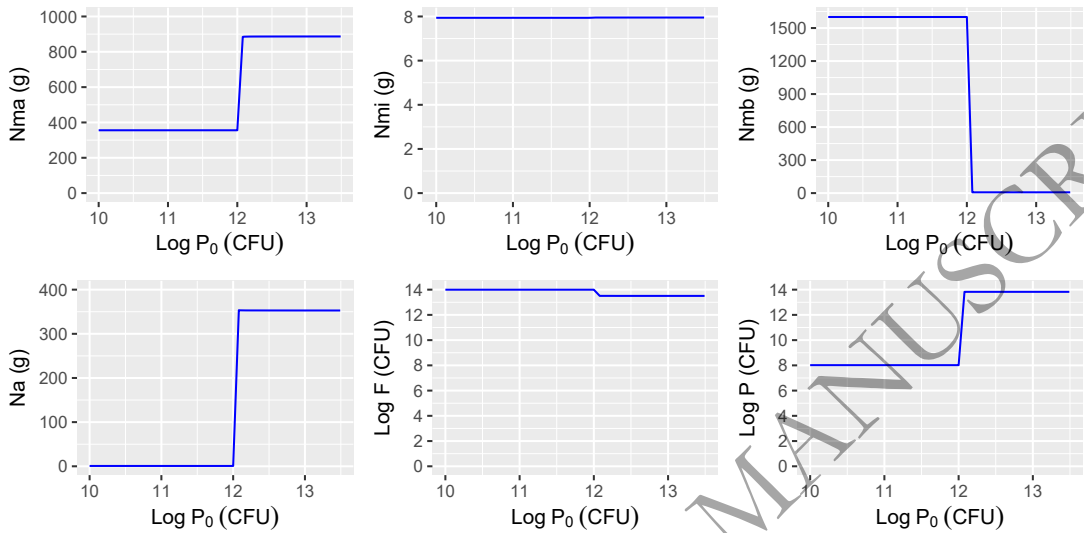


FIG. 5. The predicted steady state concentrations of nutrient and bacterial populations from solving equations (2.1)-(2.6) with baseline parameters given in Table 2 with increasing initial pathogen population  $P_0$ . As before,  $E = 0.9$ ,  $C = 0.45$  pg/ml,  $M = 4.9 \times 10^5$  cells/ml,  $B = 3.8 \times 10^3$  cells/ml. Initial conditions for  $N_{ma}$ ,  $N_{mi}$ ,  $N_{mb}$ ,  $N_a$  and  $F$  are constant.

### 2.1.2. Model results for microbiota

Using the parameter values in Table 2 and solving equations (2.1)-(2.6), Figure 6 shows the predicted behaviour of the nutrient concentrations and bacteria populations over time with no probiotic supplementation and with and without inflammation. For simulations of a healthy state with no inflammation present, we assume that the concentration of pro-inflammatory cytokines  $C = 0.27$  pg/ml, densities of macrophages and plasma B cells are  $M = 3.4 \times 10^5$  cells/ml and  $B = 2.6 \times 10^3$  cells/ml, respectively, with no damaged epithelial cells, i.e.  $E = 1$ . Under inflammatory conditions,  $C$ ,  $M$  and  $B$  are upregulated and  $E$  is downregulated as the epithelial cells experience damage.

In a healthy individual with no inflammation, the concentration of nutrients and bacterial populations attain a steady state. The concentration of alternate nutrients  $N_a$  is small, so that the commensal bacteria dominate, utilising the metabolites and micronutrients to proliferate and inhibiting the growth of pathogenic bacteria. Under inflammatory conditions, the population of pathogenic bacteria grows, resulting in fewer commensals to consume the macronutrients (hence the concentration of  $N_{ma}$  increases) and convert them into metabolites. The concentration of metabolites therefore decreases, providing less fuel for the intestinal epithelial cells, instead favouring conversion to alternate nutrients by the pathogenic bacteria. Pathogenic bacteria then utilise these alternate nutrients to proliferate at a rate greater than the rate at which they are eliminated by AMPs and the inflammatory response. The concentration of micronutrients remains almost unchanged.

### 2.2. Vitamin D and the Vitamin D Receptor

We assume that vitamin D (25(OH)D), denoted by  $D$ , is converted in the kidney by 1- $\alpha$ -hydroxylase (CYP27B1) into its active form 1,25-dihydroxyvitamin D (1,25(OH)<sub>2</sub>D), represented by  $D_a$ . However, 1,25(OH)<sub>2</sub>D can directly inhibit expression of CYP27B1 as a safeguard mechanism

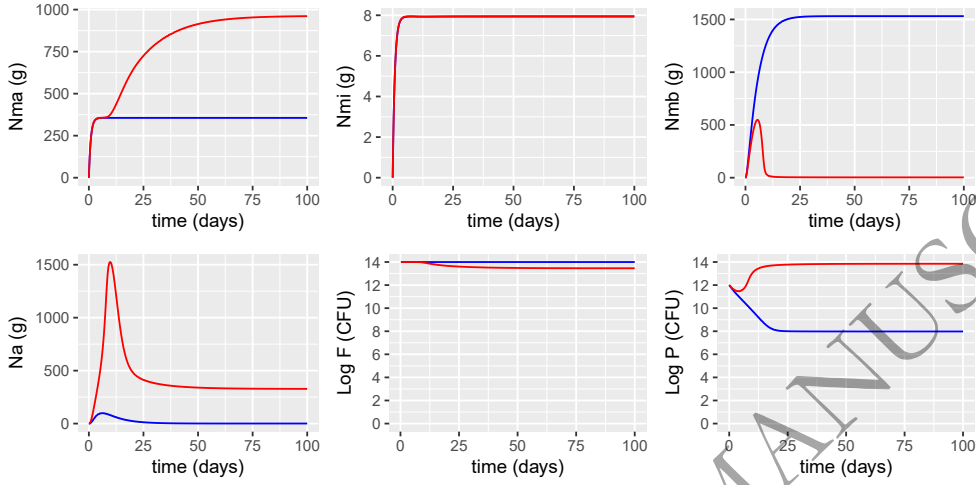


FIG. 6. Simulations predicting the concentrations of macronutrients  $N_{ma}$ , micronutrients  $N_{mi}$ , metabolites  $N_{mb}$ , alternate nutrients  $N_a$  and populations of commensals  $F$  and pathogens  $P$  from solving equations (2.1)-(2.6) with baseline parameter values given in Table 2 with (red line) and without (blue line) inflammation.  $C = 0.27$  pg/ml,  $M = 3.4 \times 10^5$  cells/ml,  $B = 2.6 \times 10^3$  cells/ml and  $E = 1$  for the non-inflammatory case and  $C = 0.91$  pg/ml,  $M = 9.8 \times 10^5$  cells/ml,  $B = 7.6 \times 10^3$  cells/ml and  $E = 0.8$  for the inflammatory case. Note that probiotic supplementation is not considered here, so  $P_b = 0$ .

222 against hypercalcaemia (Tang et al. 2019). Availability of 25(OH)D from the diet, supplements and  
 223 sunlight is denoted by  $D^0$ . In Jones et al. 2013, it was shown that probiotic supplements increase serum  
 224 concentrations of 25(OH)D in humans and can increase intestinal vitamin D absorption (Abboud et al.  
 225 2020). We therefore include a saturating term involving the probiotics with maximum production rate  
 226  $\delta_1$ . The equations governing the serum concentrations are

$$\frac{dD}{dt} = D^0 \left( 1 + \frac{\delta_1 P_b}{K_\delta + P_b} \right) - \frac{k_d D}{\delta(1 + D_a)(K_D + D)} - \delta_2 D, \quad (2.9)$$

$$\frac{dD_a}{dt} = \frac{k_d D}{\delta(1 + D_a)(K_D + D)} - \delta_3 D_a, \quad (2.10)$$

227 where  $k_d/\delta(1 + D_a)$  is the maximal rate of conversion of 25(OH)D to 1,25(OH)<sub>2</sub>D,  $K_D$  is the Michaelis-  
 228 Menten constant,  $\delta_2$  is the rate of degradation and conversion to other metabolites of 25(OH)D and  $\delta_3$   
 229 is the degradation rate of 1,25(OH)<sub>2</sub>D.

230 As discussed in Chun et al. 2012, the serum vitamin D binding protein (DBP - this is the main serum  
 231 carrier of vitamin D metabolites) and to a lesser extent, albumin, play a key role in the bioavailability  
 232 of 25(OH)D and 1,25(OH)<sub>2</sub>D. Some functions of vitamin D are more closely correlated with levels of  
 233 free 25(OH)D, rather than the total serum concentration. We therefore assume that the concentrations  
 234 of free 25(OH)D and 1,25(OH)<sub>2</sub>D, denoted by  $D_f$  and  $D_{a_f}$ , respectively, are given by

$$D_f = \mu_f D, \quad D_{a_f} = \mu_{a_f} D_a \quad (2.11)$$

235 where  $\mu_f$  and  $\mu_{a_f}$  denote the proportions of total 25(OH)D and 1,25(OH)<sub>2</sub>D that are free. Data presented  
 236 in Chun et al. 2012 showed that for a physiological concentration of serum 25(OH)D (50 nM) and

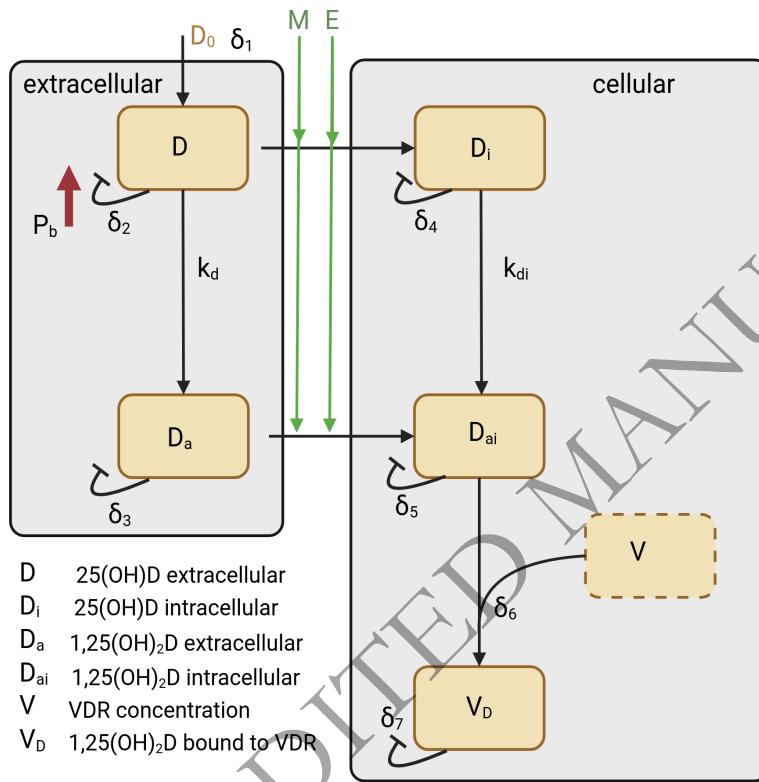


FIG. 7. **The vitamin D network.** The model derived in equations (2.9)-(2.14) describes the conversion of 25(OH)D into its active form 1,25(OH)<sub>2</sub>D, the diffusion of the free forms of these across the epithelial and macrophage cell membranes and the binding with the vitamin D receptor. The rates are defined in Table 3.

237 1,25(OH)<sub>2</sub>D (100 pM), the percentage of free 25(OH)D and 1,25(OH)<sub>2</sub>D *in vivo* ranged from 0.026-  
 238 0.074% and 0.4-1.3%, respectively.

239 We assume that free vitamin D and its metabolites can diffuse across the membrane from the  
 240 extracellular space into the intracellular fluid of macrophages and vice versa, and likewise for epithelial  
 241 cells lining the intestinal wall. The extracellular concentrations of 25(OH)D and 1,25(OH)<sub>2</sub>D act as a  
 242 source for intracellular levels of vitamin D metabolites but as the blood volume is much larger than  
 243 the intracellular volume we assume (as in Chun et al. 2012) that the extracellular levels are little  
 244 affected by intracellular dynamics. Intracellular 25(OH)D is converted into 1,25(OH)<sub>2</sub>D via the enzyme  
 245 CYP27B1 and both 25(OH)D and 1,25(OH)<sub>2</sub>D bind to the vitamin D receptor (VDR), which functions  
 246 as a transcription factor regulating gene expression. The magnitude of this response depends upon  
 247 the concentration of ligand and receptor present. This is a key mechanism underpinning the innate  
 248 antibacterial responses. However, 25(OH)D has a 500-fold lower affinity for VDR than 1,25(OH)<sub>2</sub>D, so  
 249 we only consider the binding of 1,25(OH)<sub>2</sub>D to the VDR. The intracellular concentrations of 25(OH)D,

denoted by  $D_i$  and 1,25(OH)<sub>2</sub>D, denoted by  $D_{a_i}$  is governed by

$$\frac{dD_i}{dt} = (\mu_f D - D_i)(\sigma_1 M + \sigma_2 E) - \frac{k_{d_i} D_i}{\delta_i (1 + D_{a_i})(K_{D_i} + D_i)} - \delta_4 D_i, \quad (2.12)$$

$$\frac{dD_{a_i}}{dt} = (\mu_{f_a} D_a - D_{a_i})(\sigma_1 M + \sigma_2 E) + \frac{k_{d_i} D_i}{\delta_i (1 + D_{a_i})(K_{D_i} + D_i)} - \delta_5 D_{a_i}, \quad (2.13)$$

where  $k_{d_i}/\delta_i(1 + D_{a_i})$  is the maximal rate of conversion of intracellular 25(OH)D to 1,25(OH)<sub>2</sub>D,  $K_{D_i}$  is the Michaelis-Menten constant,  $\sigma_1$  and  $\sigma_2$  are the permeabilities of macrophages and epithelial cells, respectively, to the vitamin D metabolites,  $\delta_4$  is the rate of degradation and conversion to other metabolites of intracellular 25(OH)D and  $\delta_5$  is the degradation rate of intracellular 1,25(OH)<sub>2</sub>D.  $M$  and  $E$  represent the density of macrophages and volume fraction of epithelial cells present. It should be noted that T cells and B cells do not express VDR until they are stimulated with a mitogen or antigen (pathogenic or commensal) and, therefore, there appears to be a threshold for activation of intracellular 1,25(OH)<sub>2</sub>D (Karmali et al. 1991). However, we do not include this complexity.

We assume that  $V_{D_a}$  represents the complex VDR:1,25(OH)<sub>2</sub>D that is responsible for inducing the cellular response. The most sensitively regulated gene for 1,25(OH)<sub>2</sub>D-VDR is CYP24A1 which encodes the enzyme 24-hydroxylase. This acts as a feedback mechanism to convert 1,25(OH)<sub>2</sub>D to 1,24,25(OH)<sub>3</sub>D, which is a much less active vitamin D metabolite and binds to VDR with lower affinity (Chun et al. 2012). 1,25(OH)<sub>2</sub>D therefore actively promotes its own inactivation and we encompass this into the last term in the equation

$$\frac{dV_{D_a}}{dt} = \delta_6 D_{a_i} V - \delta_7 V_{D_a}. \quad (2.14)$$

Here  $\delta_6$  is the rate at which 1,25(OH)<sub>2</sub>D binds to the VDR,  $V$  is the concentration of VDR and  $\delta_7$  is the rate of conversion or degradation.

Probiotics increase VDR protein expression and transcriptional activity which regulates host response to invasive pathogens (i.e. upregulates function of intestinal epithelial barrier, production of AMPs from epithelial cells and immune cells and autophagy and downregulates pro-inflammatory cytokines) and commensal bacteria in innate and adaptive immunity (de Vos et al. 2017, Mujagic et al. 2017, Stojanov et al. 2020). In Lu et al. 2020 a single dose of probiotic resulted in an increase in VDR and autophagy signalling and inhibited inflammation. In our model, the concentration of VDR,  $V$ , is therefore assumed to depend upon the intake of probiotics  $P_b$  so that it takes the saturating form

$$V = \frac{\delta_8(a + P_b)}{P_b + K_V}, \quad (2.15)$$

where  $V = \delta_8 a / K_V$  when  $P_b = 0$ . A summary of these interactions is shown in Figure 7.

We assume that at time  $t = 0$  the concentration of serum 25(OH)D is constant and the concentrations of its metabolites are at steady state, i.e.

$$D_0 = D_{ss}, \quad D_{a_0} = D_{a_{ss}}, \quad D_{i_0} = D_{i_{ss}}, \quad D_{a_{i_0}} = D_{a_{i_{ss}}}, \quad V_{D_{a_0}} = V_{D_{a_{ss}}}. \quad (2.16)$$

### 2.2.1. Parameter values and sensitivity analysis for vitamin D model

Most parameter values are available from Chun et al. 2012 and Beetjes et al. 2019. The remainder were estimated to obtain results similar to measurements from experimental studies in the literature. A summary of values with units and references is given in Table 3.



Parameter	Description	Value & Units	Reference
$D^0$	Production of 25(OH)D from diet and sunlight	variable nM/day	
$k_d/\delta$	Maximal rate of conversion of extracellular 25(OH)D to 1,25(OH) <sub>2</sub> D	24 nM/day	Chun et al. 2012
$K_D$	Michaelis Menten constant for extracellular 25(OH)D binding to CYP27B1	1000 nM	Chun et al. 2012
$\delta_1$	$D^0 \delta_1$ is the maximum production rate of vitamin D dependent upon probiotics	0.3	
$\delta_2$	Degradation of extracellular 25(OH)D	0.048 day <sup>-1</sup>	Beetjes et al. 2019
$\delta_3$	Degradation of extracellular 1,25(OH) <sub>2</sub> D	14.4 day <sup>-1</sup>	Beetjes et al. 2019
$\mu_f$	Proportion of total extracellular 25(OH)D that is free	0.05 %	Chun et al. 2012
$\mu_{a_f}$	Proportion of total extracellular 1,25(OH) <sub>2</sub> D that is free	0.85 %	Chun et al. 2012
$\sigma_1$	Permeability of macrophages to free 25(OH)D or 1,25(OH) <sub>2</sub> D	144 day <sup>-1</sup>	Chun et al. 2012
$\sigma_2$	Permeability of epithelial cells to free 25(OH)D or 1,25(OH) <sub>2</sub> D	144 day <sup>-1</sup>	
$k_{d_i}/\delta$	Maximal rate of conversion of intracellular 25(OH)D to 1,25(OH) <sub>2</sub> D	24 nM/day	Chun et al. 2012
$K_{D_i}$	Michaelis Menten constant for intracellular 25(OH)D binding to CYP27B1	1000 nM	Chun et al. 2012
$\delta_4$	Degradation of intracellular 25(OH)D	0.048 day <sup>-1</sup>	Beetjes et al. 2019
$\delta_5$	Degradation of intracellular 1,25(OH) <sub>2</sub> D	14.4 day <sup>-1</sup>	Beetjes et al. 2019
$\delta_6$	Rate at which 1,25(OH) <sub>2</sub> D binds to VDR	$24 \times 10^{-7}$ nM <sup>-1</sup> day <sup>-1</sup>	Chun et al. 2012
$\delta_7$	Rate of degradation of VDR:1,25(OH) <sub>2</sub> D	0.024 day <sup>-1</sup>	
$\delta_8 a/K_V$	Concentration of VDR	1.2 nM	Chun et al. 2012
$K_V$	Saturation constant	1 CFU/day	
$K_\delta$	Saturation constant	$5 \times 10^8$ CFU/day	

TABLE 3 Definition, value and units of the vitamin D model parameters. Note that 1 nM of 25(OH)D = 2.5 ng/ml.

Employing a similar method to that described in Subsection 2.1.1, using constant values for the volume fraction of healthy epithelial cells  $E$  and macrophage density  $M$ , indicates that the concentration of vitamin D and its metabolites is dependent upon several different parameters (see Figure 8). All of the variables are sensitive to the rate of intake of 25(OH)D by diet and sunlight  $D^0$ , the maximum production rate of vitamin D dependent upon probiotics  $\delta_1$ , the degradation of 25(OH)D  $\delta_2$ , the Michaelis-Menten constant for extracellular 25(OH)D binding to CYP27B1  $K_D$  and the maximal rate of conversion of extracellular 25(OH)D to 1,25(OH)<sub>2</sub>D  $k_d$ . The intracellular and extracellular concentrations of 1,25(OH)<sub>2</sub>D and VDR:1,25(OH)<sub>2</sub>D complex are also dependent upon the degradation rate of 1,25(OH)<sub>2</sub>D  $\delta_3$ . The intracellular metabolites  $D_i$  and  $D_{a_i}$  are influenced by the proportion of their extracellular versions that are free i.e.  $\mu_f$  and  $\mu_{a_f}$ , respectively. The concentration of the VDR:1,25(OH)<sub>2</sub>D complex is also sensitive to the latter, in addition to the rate at which 1,25(OH)<sub>2</sub>D binds to VDR  $\delta_6$ , the rate of degradation of VDR:1,25(OH)<sub>2</sub>D  $\delta_7$  and the concentration of VDR  $\delta_8$ . None of the variables depend upon  $s = \sigma_1 = \sigma_2$ , which could be interpreted as the change in the term  $M + E$ , and the model is insensitive to changes in initial conditions.

### 2.2.2. Model results for vitamin D/VDR pathway

We solve equations (2.9)-(2.14) using the parameter values given in Table 3 for vitamin D and its metabolites. Vitamin D intake  $D^0$  is chosen to represent production of 25(OH)D from diet and sunlight

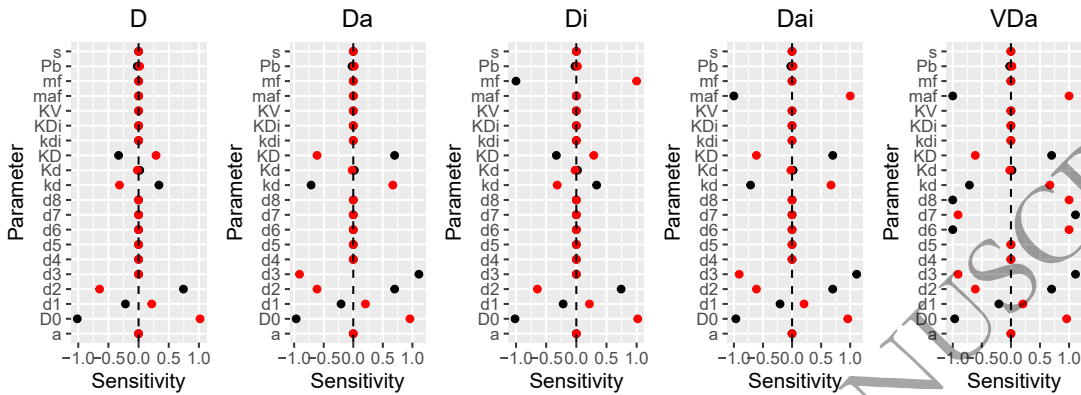


FIG. 8. The effect on varying parameter values on the steady state concentrations of extra- and intra-cellular 25(OH)<sub>2</sub>D, 1,25(OH)<sub>2</sub>D and the complex VDR:1,25(OH)<sub>2</sub>D. Baseline parameter values are taken from Table 3 and each parameter is sequentially varied by a 10% decrease (black) and a 10% increase (red). Sensitivity is defined by equation (2.8) and  $s$  represents the permeability of macrophages and epithelial cells to 25(OH)<sub>2</sub>D and 1,25(OH)<sub>2</sub>D i.e.  $s = \sigma_1 = \sigma_2$ . The volume fraction of epithelial cells  $E = 0.9$  and density of macrophages  $M = 4.9 \times 10^5$  cells/ml. Note that  $m = \mu$  and  $d = \delta$ .

298 only (no supplements) and  $P_b = 0$ , representing no daily supplement of probiotics. Figure 9 shows the  
 299 predicted concentrations over time with and without inflammation.

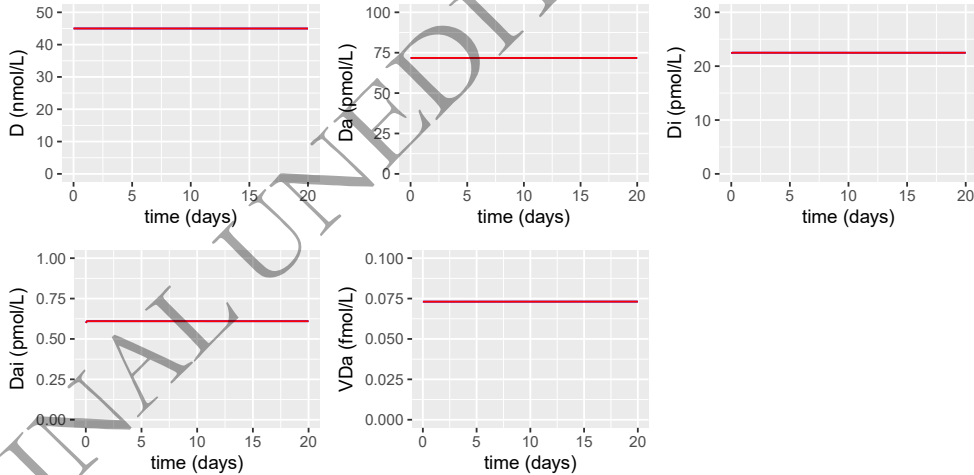


FIG. 9. Simulations predicting the effect of inflammation on the concentrations of extracellular and intracellular 25(OH)<sub>2</sub>D and 1,25(OH)<sub>2</sub>D and of the VDR:1,25(OH)<sub>2</sub>D complex from solving equations (2.9)-(2.14) with baseline parameter values given in Table 3. The density of macrophages increases from  $M = 3.4 \times 10^5$  (blue) to  $M = 9.8 \times 10^5$  cells/ml (red) and the volume fraction of healthy epithelial cells decreases from  $E = 1$  (blue) to  $E = 0.8$  (red). Supplementation is not considered here, so  $P_b = 0$  and  $D^0 = 3.2$  nM/day (8 ng/ml day<sup>-1</sup>), which represents intake of vitamin D from diet and sunlight only.

300 Under non-inflammatory conditions (i.e. when the density of macrophages  $M = 3.4 \times 10^5$  cells/ml  
 301 and the volume fraction of healthy epithelial cells  $E = 1$ ), the concentrations of serum and intracellular

25(OH)D and 1,25(OH)<sub>2</sub>D and VDR:1,25(OH)<sub>2</sub>D complex remain constant. As reported in Tang et al. 2019 and Souberbielle et al. 2016, there is an approximate 1000-fold difference between the serum concentrations of 25(OH)D and its metabolite, which is also predicted by our model. Under inflammatory conditions, the density of macrophages  $M$  increases and the volume fraction of healthy epithelial cells decreases so that  $M > 3.4 \times 10^5$  and  $E < 1$ . This increases the magnitude of the term  $(\sigma_1 M + \sigma_2 E)$  as there are overall more cells which 25(OH)D and 1,25(OH)<sub>2</sub>D can enter and bind to the vitamin D receptor. The local sensitivity analysis presented in Section 2.2.1 suggests that an increase in this term has a negligible effect on the levels of 25(OH)D and its metabolites. This is also demonstrated in Figure 9.

### 2.3. The intestinal epithelial barrier and the immune response

We recall that epithelial cells are either healthy or damaged, so that the sum of their volume fractions

$$E + E_d = 1. \quad (2.17)$$

SCFAs (metabolites) provide energy for the proliferation of epithelial cells at rate  $\epsilon_1$  and VDR expression (which is enhanced by probiotics) upregulates the epithelial barrier function at rate  $\epsilon_2$  through induction of genes encoding tight junction components. However, pro-inflammatory mediators and toxins from inflowing pathogenic bacteria damage the epithelial cells at rate  $\epsilon_4$  and  $\epsilon_5$ , respectively, with macrophages removing damaged cells at rate  $\epsilon_3$ . We therefore have

$$\frac{dE}{dt} = \epsilon_1 N_{mb} E_d + (\epsilon_2 V_{D_a} + \epsilon_3 M) E_d - \epsilon_4 C E - \epsilon_5 P E, \quad (2.18)$$

$$\frac{dE_d}{dt} = \epsilon_4 C E + \epsilon_5 P E - (\epsilon_2 V_{D_a} + \epsilon_3 M) E_d - \epsilon_1 N_{mb} E_d \quad (2.19)$$

The microbiota are involved in the training and development of major components of the host's innate and adaptive immune systems (Zheng et al. 2020). A multitude of immune cells play a role in maintaining the integrity of the intestinal barrier and the model is restricted to include macrophages (density  $M$ ), T-helper cells (density  $T_h$ ), plasma B cells (density  $B$ ) and a combined regulatory T and B cell density term  $R$ , which dampens down the immune response. It is important to include all these individual cell terms due to their specific functions in modifying, via the vitamin D receptor, the immune response. For example (as detailed in Subsection 2.2 and the model formulation below), antigen-presenting cells such as macrophages intracellularly convert 25(OH)D to active 1,25(OH)<sub>2</sub>D. This may then act locally (intracrine) to modify macrophage function via the vitamin D receptors expressed by the same cells. The VDR:1,25(OH)<sub>2</sub>D complex released by macrophages may also affect adjacent T and B cells by promoting regulatory cell function and inhibiting T-helper and plasma B cell proliferation (Lopez et al. 2021). The model has been established to incorporate these cell-specific differences.

Epithelial and immune cells release a variety of chemokines and cytokines that have a range of functions. We consider here generic pro-inflammatory-type and anti-inflammatory-type cytokines denoted by  $C$  and  $G$ , respectively. A summary of the interactions between these components is shown in Figure 10.

*Innate immune response.* Intestinal mucosal macrophages are positioned in the subepithelial lamina propria where they can regulate inflammatory responses to bacteria that breach the epithelium, protect the mucosa against harmful pathogens, and scavenge dead cells and foreign debris (Smith et al. 2011). These macrophages exhibit greater phagocytic ability than other macrophages and under healthy

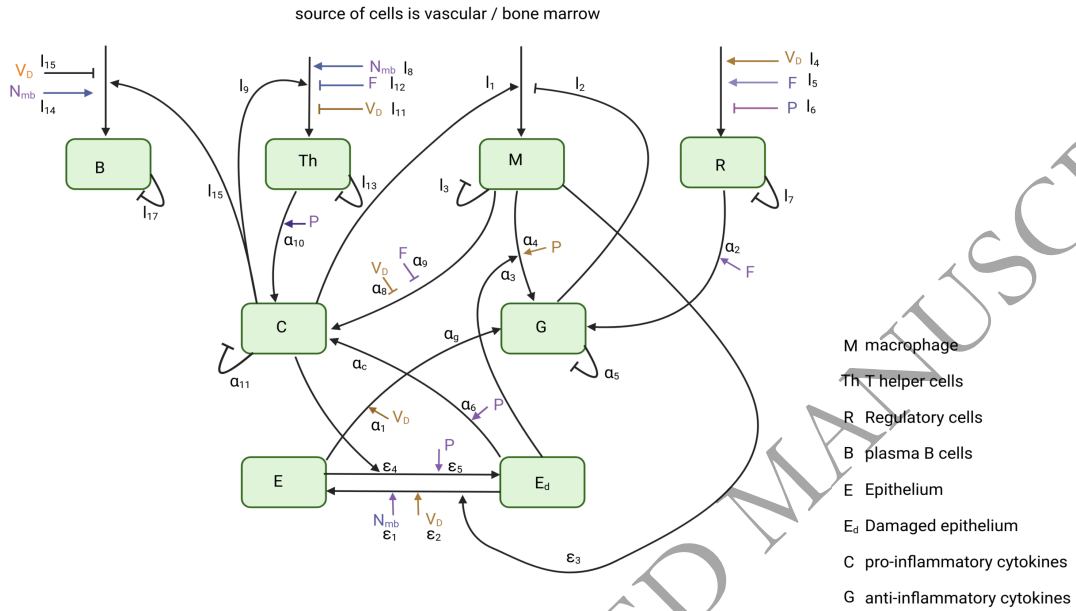


FIG. 10. **The immune response network.** The model derived in equations (2.18)-(2.25) details the interactions between the intestinal epithelial barrier and the innate and adaptive immune responses. The parameters are defined in Tables 4 and 5.

338 conditions lack the normal pro-inflammatory cytokine release that can be switched in disease (Smith et  
 339 al. 2011). Pathogenic bacteria stimulate priming of intestinal macrophages through pro-inflammatory  
 340 cytokines (rate  $l_1$ ) that promote recruitment of neutrophils to the site of infection which eradicate the  
 341 pathogens. Macrophages are long lived, dying (or migrating) after weeks or months (rate  $l_3$ ), this rate  
 342 increasing under inflammatory conditions (De Maeyer et al. 2021). Newly arriving macrophages have  
 343 a more pro-inflammatory phenotype in the elderly that is reduced under the effect of anti-inflammatory  
 344 mediators, rate  $l_2$  (De Maeyer et al. 2021). Vitamin D impairs the activation of macrophages as an  
 345 increase in VDR expression downregulates the pro-inflammatory cytokines. The equation for  $M$  is thus

$$\frac{dM}{dt} = l_1 C - l_2 G M - l_3 M. \quad (2.20)$$

346 *T and B cells.* Naive T cells ( $T$ ) differentiate into the subpopulations, regulatory T cells (Tregs) and Th  
 347 (consisting of Th17, Th1 and Th2) cells, favouring the development of Tregs in the presence of VDR.  
 348 Commensal bacteria and probiotics also promote Tregs differentiation but, conversely, pathogenic  
 349 bacteria downregulate Tregs (Yamamoto et al. 2020).

350 B cells are, like T cells, part of the adaptive immune response. They are in the blood and lymph  
 351 nodes, as well as in the intestinal mucosa. B cells differentiate into several subpopulations: of interest  
 352 here are the plasma B cells, which produce IgA, and regulatory B cells Bregs, which, like Tregs, dampen  
 353 down the immune response (Yamamoto et al. 2020). Specific probiotics can also affect differentiation  
 354 (Cristofori et al. 2021) but we do not consider this mechanism here. We combine Tregs and Bregs into

355 one variable denoted by  $R$  that satisfies the equation

$$\frac{dR}{dt} = \frac{(\iota_4 V_{D_a} + \iota_5 F)}{1 + \iota_6 P} - \iota_7 R, \quad (2.21)$$

356 where  $\iota_4$  and  $\iota_5$  denote the rates that T cells and B cells differentiate into regulatory T and B cells in  
 357 the presence of VDR and commensal bacteria, respectively.  $\iota_6$  is the rate at which differentiation into  
 358 regulatory cells is inhibited by pathogenic bacteria and  $\iota_7$  is their combined natural death rate.

359 Antigen-specific T cells proliferate and are activated at the site of contact in response to pathogenic  
 360 bacteria (rate  $\iota_{10}$ ) and high concentrations of pro-inflammatory cytokines (rate  $\iota_9$ ). They also utilise  
 361 metabolites for proliferation (rate  $\iota_8$ ). However, VDR, probiotics and commensal bacteria can inhibit T  
 362 cell proliferation and pro-inflammatory cytokine production. Hence

$$\frac{dT_h}{dt} = \frac{(\iota_8 N_{mb} + \iota_9 C + \iota_{10} P)}{(1 + \iota_{11} V_{D_a} + \iota_{12} F)} - \iota_{13} T_h, \quad (2.22)$$

363 where  $\iota_{13}$  is the natural death rates of  $T_h$  cells.

364 B cells are activated at rate  $\iota_{14}$  by taking up bacterial products (metabolites). Th cells make pro-  
 365 inflammatory cytokines to help B cells mature (rate  $\iota_{15}$ ) to make antibodies, specifically IgA. Vitamin  
 366 D impairs the activation of macrophages and B cells (rate  $\iota_{16}$ ) and low serum levels of 25(OH)D have  
 367 been shown to be inversely correlated with IgA (Yamamoto et al. 2020). The equation governing plasma  
 368 B cells is thus

$$\frac{dB}{dt} = \frac{\iota_{14} N_{mb} + \iota_{15} C}{1 + \iota_{16} V_{D_a}} - \iota_{17} B, \quad (2.23)$$

369 where  $\iota_{17}$  is the natural death rates of B cells.

370 *Pro- and anti-inflammatory mediators.* VDR expression upregulates anti-inflammatory cytokines  
 371 produced by epithelial cells at rate  $\alpha_1$  (Abboud et al. 2020). Commensal bacteria stimulate anti-  
 372 inflammatory cytokine production by regulatory T and B cells at rate  $\alpha_2$ . Macrophages also produce  
 373 anti-inflammatory cytokines after consuming damaged epithelial cells (rate  $\alpha_3$ ) and pathogens (rate  $\alpha_4$ )  
 374 (Yamamoto et al. 2020). The dynamics of the anti-inflammatory cytokines is then

$$\frac{dG}{dt} = \gamma_g + (\alpha_g + \alpha_1 V_{D_a})E + \alpha_2 FR + (\alpha_3 E_d + \alpha_4 P)M - \alpha_5 G, \quad (2.24)$$

375 where  $\alpha_5$  is the natural degradation rate and intestinal epithelial cells release anti-inflammatory  
 376 cytokines at a low-level background rate  $\alpha_g$ .  $\gamma_g$  represents the background production of anti-  
 377 inflammatory cytokines by other cells.

378 Pro-inflammatory cytokines are released when the epithelial cells are stressed (due to pathogenic  
 379 bacteria at rate  $\alpha_6 E_d P$ ). VDR reduces pro-inflammatory cytokines (rate  $\alpha_8$ ) and it has been shown  
 380 that a deficiency of VDR expression in macrophages and granulocytes results in an increase in pro-  
 381 inflammatory cytokines (Nielsen et al. 2018). Further production of pro-inflammatory cytokines is  
 382 carried out by activated innate immune cells (rate  $\alpha_7$ ) and by Th cells in response to the pathogenic  
 383 bacteria (rate  $\alpha_{10}$ ). Commensal bacteria lead to a downregulation of pro-inflammatory cytokine  
 384 production by macrophages, rate  $\alpha_9$ . Regulatory cells also dampen down their production by increasing  
 385 the concentration of anti-inflammatory cytokines that decrease the macrophage density (Yamamoto et

386 al. 2020). Hence

$$\frac{dC}{dt} = \gamma_c + (\alpha_c + \alpha_6 P)E_d + \frac{\alpha_7 M}{(1 + \alpha_8 V_{D_a} + \alpha_9 F)} + \alpha_{10} P T_h - \alpha_{11} C, \quad (2.25)$$

387 where  $\alpha_{11}$  is the natural pro-inflammatory cytokine decay rate and damaged intestinal epithelial cells  
388 release pro-inflammatory cytokines at a low-level background rate  $\alpha_c$ .  $\gamma_c$  represents the background  
389 production of pro-inflammatory cytokines by other cells.

390 We assume initially, at time  $t = 0$ , that the epithelial barrier is healthy and the density of immune  
391 cells is at steady state:

$$E_0 = 1, \quad E_{d_0} = 0, \quad M_0 = M_{ss}, \quad R_0 = R_{ss}, \quad T_{h_0} = T_{h_{ss}}, \quad B_0 = B_{ss}, \quad G_0 = G_{ss}, \quad C_0 = C_{ss}. \quad (2.26)$$

392 where subscript  $_{ss}$  denotes the immune cell densities at steady state.

### 393 2.3.1. Parameter values and sensitivity for immune response model

394 All the parameters in this sub-model are unknown but estimates are given in Tables 4 and 5.

Parameter	Description	Value	Units
$\epsilon_1$	Proliferation rate of intestinal epithelial cells	$4.9 \times 10^{-13}$	(ng.day) <sup>-1</sup>
$\epsilon_2$	Rate of repair of damaged epithelial cells by VDR	$2 \times 10^9$	ml/(ng.day)
$\epsilon_3$	Removal rate of damaged epithelial cells by macrophages	$3.17 \times 10^{-6}$	ml/day
$\epsilon_4$	Damage to epithelial cells by pro-inflammatory mediators	$2.7 \times 10^3$	ml/(ng.day)
$\epsilon_5$	Damage to epithelial cells by pathogenic bacteria	$1 \times 10^{-12}$	(CFU.day) <sup>-1</sup>

TABLE 4 *Definition, baseline values and units for the epithelial barrier model parameters.*

395 Given the lack of information on the parameters, the sensitivity analysis is particularly important  
396 for this sub-model. We use constant values for the bacterial populations  $F$  and  $P$ , the concentration of  
397 metabolites  $N_{mb}$  and the concentration of the VDR:1,25(OH)<sub>2</sub>D complex  $V_{D_a}$  and implement a similar  
398 method to that described in Subsection 2.1.1 to assess the sensitivity of the model to local changes in  
399 the baseline parameters given in Tables 4 and 5. The sensitivity plots are presented in Figure 11.

400 The volume fraction of healthy and damaged epithelial cells is sensitive to the rates of repair of  
401 damaged epithelial cells by VDR and of damage to epithelial cells by pathogenic bacteria,  $\epsilon_2$  and  $\epsilon_5$ ,  
402 respectively. These two parameters also influence the density of macrophages and plasma B cells and  
403 the concentration of anti- and pro-inflammatory cytokines, along with the natural degradation of pro-  
404 inflammatory cytokines  $\alpha_{11}$  and the rate of pro-inflammatory cytokine release by damaged epithelial  
405 cells  $\alpha_c$ . A decrease in the death rate of macrophages  $\iota_3$  and an increase in the rate of activation  
406 of macrophages by pro-inflammatory cytokines  $\iota_1$  results in an increase in macrophages and anti-  
407 inflammatory cytokines. The latter is also influenced by its production rate by macrophages after  
408 consuming pathogenic bacteria  $\alpha_4$  and the rate that T and B cells are differentiated into regulatory  
409 cells in the presence of commensal bacteria  $\iota_5$ . Also of note is the sensitivity of plasma B cells to their  
410 rate of maturation in the presence of pro-inflammatory cytokines  $\iota_{15}$ , the rate of their inhibition by VDR  
411  $\iota_{16}$  and their natural death rate  $\iota_{17}$ . Regulatory cells are sensitive to a decrease in their death rate  $\iota_7$   
412 and changes to the rate of their production in the presence of VDR  $\iota_4$ . Finally, a decrease in the rates of  
413 inhibition to Th cell proliferation by VDR  $\iota_{11}$  and natural death of Th cells  $\iota_{13}$  and an increase in the



Parameter	Description	Value	Units
$t_1$	Rate of activation of macrophages by pro-inflammatory cytokines	$1.35 \times 10^9$	$(\text{ng.day})^{-1}$
$t_2$	Rate of inhibition of macrophages by anti-inflammatory cytokines	$1.13 \times 10^2$	$\text{ml}/(\text{ng.day})$
$t_3$	Natural death rate of macrophages	1	$\text{day}^{-1}$
$t_4$	Rate that T/B cells are differentiated into T/B regulatory cells in presence of VDR	$2.38 \times 10^{11}$	$(\text{ng.day})^{-1}$
$t_5$	Rate that T/B cells are differentiated into T/B regulatory cells in presence of commensal bacteria	$8.5 \times 10^{-11}$	$(\text{CFU.ml.day})^{-1}$
$t_6$	Rate at which differentiation into regulatory cells is inhibited by pathogenic bacteria	$1 \times 10^{-14}$	$\text{CFU}^{-1}$
$t_7$	Combined natural death rate of T/B regulatory cells	1	$\text{day}^{-1}$
$t_8$	Rate of utilisation of metabolites for T-helper cell proliferation	$2.57 \times 10^{-8}$	$(\text{ng.ml.day})^{-1}$
$t_9$	Rate of T-helper cell proliferation in response to pro-inflammatory cytokines	$1.12 \times 10^9$	$(\text{ng.day})^{-1}$
$t_{10}$	Rate of T-helper cell proliferation in response to pathogenic bacteria	$1.05 \times 10^{-7}$	$(\text{CFU.ml.day})^{-1}$
$t_{11}$	Rate of inhibition to T helper cell proliferation by VDR	$4 \times 10^6$	$\text{ml}/\text{ng}$
$t_{12}$	Rate of inhibition to T helper cell proliferation by commensals	$1 \times 10^{-15}$	$\text{CFU}^{-1}$
$t_{13}$	Natural rate of T-helper cell death	10	$\text{day}^{-1}$
$t_{14}$	Rate of activation of plasma B cells by bacterial products	$1.28 \times 10^{-8}$	$(\text{ng.ml.day})^{-1}$
$t_{15}$	Rate of maturation of plasma B cells in presence of pro-inflammatory cytokines	$5 \times 10^8$	$(\text{ng.day})^{-1}$
$t_{16}$	Rate of inhibition of plasma B cells by VDR	$4 \times 10^8$	$\text{ml}/\text{ng}$
$t_{17}$	Natural death rate of plasma B cells	0.81	$\text{day}^{-1}$
$\alpha_1$	Production rate of anti-inflammatory cytokines by epithelial cells upregulated by VDR	$7.08 \times 10^5$	$\text{day}^{-1}$
$\alpha_2$	Production rate of anti-inflammatory cytokines by T and B regulatory cells stimulated by commensal bacteria	$2.07 \times 10^{-21}$	$\text{ng}/(\text{CFU.day})$
$\alpha_3$	Production rate of anti-inflammatory cytokines by macrophages after consuming damaged epithelial cells	$1.13 \times 10^{-7}$	$\text{ng}/\text{day}$
$\alpha_4$	Production rate of anti-inflammatory cytokines by macrophages after consuming pathogenic bacteria	$1.69 \times 10^{-20}$	$\text{ng}/(\text{CFU.day})$
$\alpha_5$	Natural degradation rate of anti-inflammatory cytokines	$7.5 \times 10^2$	$\text{day}^{-1}$
$\alpha_6$	Production rate of pro-inflammatory cytokines in response to damaged epithelial cells	$9.3 \times 10^{-18}$	$\text{ng}/(\text{CFU.ml.day})$
$\alpha_7$	Production rate of pro-inflammatory cytokines by activated innate immune cells	$5.94 \times 10^{-11}$	$\text{ng}/\text{day}$
$\alpha_8$	Inhibition of pro-inflammatory cytokines by VDR	$4 \times 10^7$	$\text{ml}/\text{ng}$
$\alpha_9$	Inhibition of pro-inflammatory cytokines by commensals	$5 \times 10^{-15}$	$\text{CFU}^{-1}$
$\alpha_{10}$	Production rate of pro-inflammatory cytokines by T helper cells	$8.78 \times 10^{-24}$	$\text{ng}/(\text{CFU.day})$
$\alpha_{11}$	Natural degradation rate of pro-inflammatory cytokines	1.2	$\text{day}^{-1}$
$\alpha_c$	Rate of pro-inflammatory cytokine release by damaged epithelial cells	$2.3 \times 10^{-3}$	$\text{ng}/(\text{ml.day})$
$\alpha_h$	Rate of anti-inflammatory cytokine release by healthy epithelial cells	$1.77 \times 10^{-3}$	$\text{ng}/(\text{ml.day})$
$\gamma_c$	Background production rate of pro-inflammatory cytokines	$3.24 \times 10^{-4}$	$\text{ng}/(\text{ml.day})$
$\gamma_g$	Background production rate of anti-inflammatory cytokines	0.35	$\text{ng}/(\text{ml.day})$

TABLE 5 Definition, baseline values and units for the immune response model parameters.

rate of Th cell proliferation in response to pro-inflammatory cytokines  $t_{10}$  results in an increase in the density of Th cells.

The sensitivity of the model to the variables  $N_{mb}$ ,  $F$ ,  $P$  and  $V_{Da}$  is shown in Figure 12. To ensure that the total population of bacteria ( $F + P$ ) does not exceed its maximum value of  $1 \times 10^{14}$  we consider a 1%



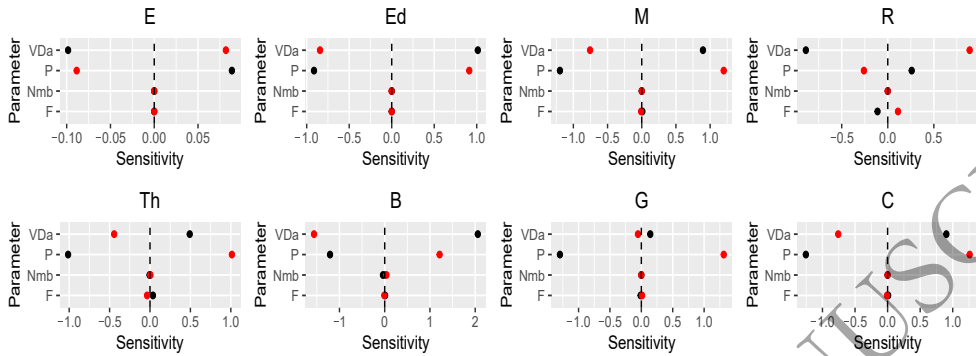


FIG. 12. The effect of varying parameter values on the steady state volume fractions of healthy and damaged epithelial cells, densities of immune cells and concentrations of pro and anti-inflammatory mediators. Baseline parameter values are taken from Tables 4 and 5 with  $N_{mb}$  and  $V_{Da}$  sequentially varied by a 10% decrease (black) and a 10% increase (red).  $F$  and  $P$  are sequentially varied by a 1% decrease (black) and a 1% increase (red). Sensitivity is defined by equation (2.8).

2.3.2. Model results for immune response

We solve equations (2.18)-(2.25) using the parameter values in Tables 4 and 5 to predict the time evolution of epithelial cells, immune cells and inflammatory mediators. We assume constant values for the commensal and pathogenic bacteria and the concentrations of metabolites and of the VDR:1,25(OH)<sub>2</sub>D complex, based on the steady state values predicted in the previous two sections with and without inflammation.

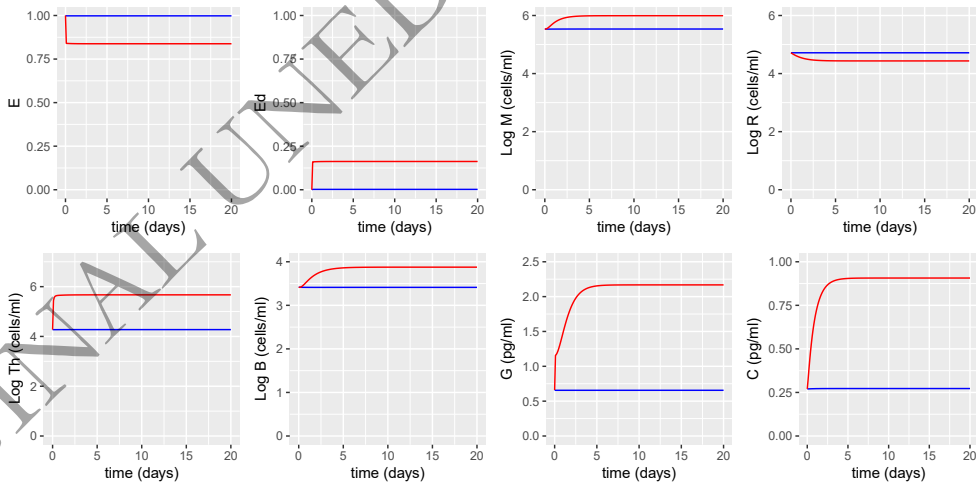


FIG. 13. Simulations predicting the volume fraction of healthy  $E$  and damaged epithelial cells  $E_d$ , the densities of macrophages  $M$ , regulatory cells  $R$ , Th cells  $T_h$  and plasma B cells  $B$  and the concentrations of anti- and pro-inflammatory cytokines,  $G$  and  $C$ , from solving equations (2.18)-(2.25) with baseline parameters given in Tables 4 and 5. Values for  $V_{Da}$ ,  $N_{mb}$ ,  $F$  and  $P$  have been taken from the steady state solutions with and without inflammation predicted in Figures 6 and 9 i.e.  $V_{Da} = 1.83 \times 10^{-7}$  ng/ml,  $N_{mb} = 1530$  g,  $F = 9.94 \times 10^{13}$  CFU,  $P = 9.6 \times 10^7$  CFU (blue) and  $V_{Da} = 1.83 \times 10^{-7}$  ng/ml,  $N_{mb} = 3.4$  g,  $F = 3 \times 10^{13}$  CFU,  $P = 6.9 \times 10^{13}$  CFU (red).

431 Figure 13 illustrates the dependence of the epithelial and immune cells on the concentration of  
432 metabolites, populations of bacteria and the VDR:1,25(OH)<sub>2</sub>D complex. As  $N_{mb}$  decreases, the volume  
433 fraction of healthy epithelial cells very quickly decreases as metabolites provide energy for their  
434 proliferation. This results in an increase in damaged epithelial cells that are under stress, increasing  
435 signalling of pro-inflammatory cytokines that upregulate the density of macrophages, Th and plasma  
436 B cells. The concentration of anti-inflammatory cytokines also increases as they attempt to counteract  
437 the effects of the pro-inflammatory mediators. The density of regulatory cells decreases as pathogenic  
438 bacteria downregulate their production.

#### 439 2.4. Sensitivity analysis for integrated model

440 The three models described by equations (2.1)-(2.26) are now combined so that quantities treated as  
441 constant in the sub-models, now vary and are determined from their ODE. A similar method to that  
442 described in Subsection 2.1.1 is used to assess the sensitivity of the integrated model. Sensitivity plots  
443 for the bacterial populations, VDR:1,25(OH)<sub>2</sub>D complex, volume fraction of healthy epithelial cells  
444 and concentration of pro-inflammatory cytokines are presented in Figures 31-33 in Appendix A.

445 Sensitivity of the model to local changes in the baseline parameters given in Tables 2-5 indicates  
446 that the parameters influencing the bacterial populations, concentrations of nutrients, concentrations  
447 of 25(OH)D and its metabolites, volume fractions of healthy and damaged epithelial cells, densities  
448 of immune cells and cytokine concentrations are the same as for the individual sub-models described  
449 in subsections 2.1.1, 2.2.1 and 2.3.1. However, the volume fraction of healthy and damaged epithelial  
450 cells, densities of immune cells and cytokine concentrations are additionally dependent upon parameters  
451 influencing the populations of pathogenic bacteria and the VDR:1,25(OH)<sub>2</sub>D complex. This is  
452 consistent with the sensitivity analysis performed in Figure 12 for the immune sub-model, which  
453 showed that the immune variables had a high dependence on  $P$  and  $V_{D_a}$ . Figure 32 suggests that  
454 the commensal and pathogenic bacterial populations, concentrations of VDR:1,25(OH)<sub>2</sub>D and pro-  
455 inflammatory cytokines and volume fraction of healthy epithelial cells are insensitive to small doses  
456 of probiotics. Similarly, the bacterial populations are not influenced by low levels of vitamin D  
457 supplementation. However, an increase in vitamin D intake results in an increase in VDR:1,25(OH)<sub>2</sub>D  
458 and healthy epithelial cells and a decrease in pro-inflammatory cytokines, indicating its potential  
459 therapeutic benefits.

460 The sensitivity of the full model to the initial conditions is also the same as for the individual sub-  
461 models, where the steady state values of the model variables are only influenced by changes in the  
462 initial pathogen population  $P_0$  (see Figure 14). As in section 2.1.1, the system is bistable so that when  
463 the initial pathogen population exceeds approximately  $0.27 \times 10^{13}$  CFU, it transitions to an inflammatory  
464 state resulting in an increase of damaged epithelial cells, signalling of pro-inflammatory cytokines and  
465 activation of immune cells.

466 The predictions for the full model are presented in the following section, where we also explore the  
467 effect of supplementation of vitamin D and probiotics on the model variables.

### 468 3. Results - Integrated model

#### 469 3.1. Model results for integrated model - no supplementation

470 We solve the full model given by equations (2.1)-(2.26) using the parameter values in Tables 2-5 to  
471 predict the time evolution of nutrients and bacteria, vitamin D and its metabolites, epithelial cells,  
472 immune cells and inflammatory mediators under normobiosis and dysbiosis. We assume that dysbiosis

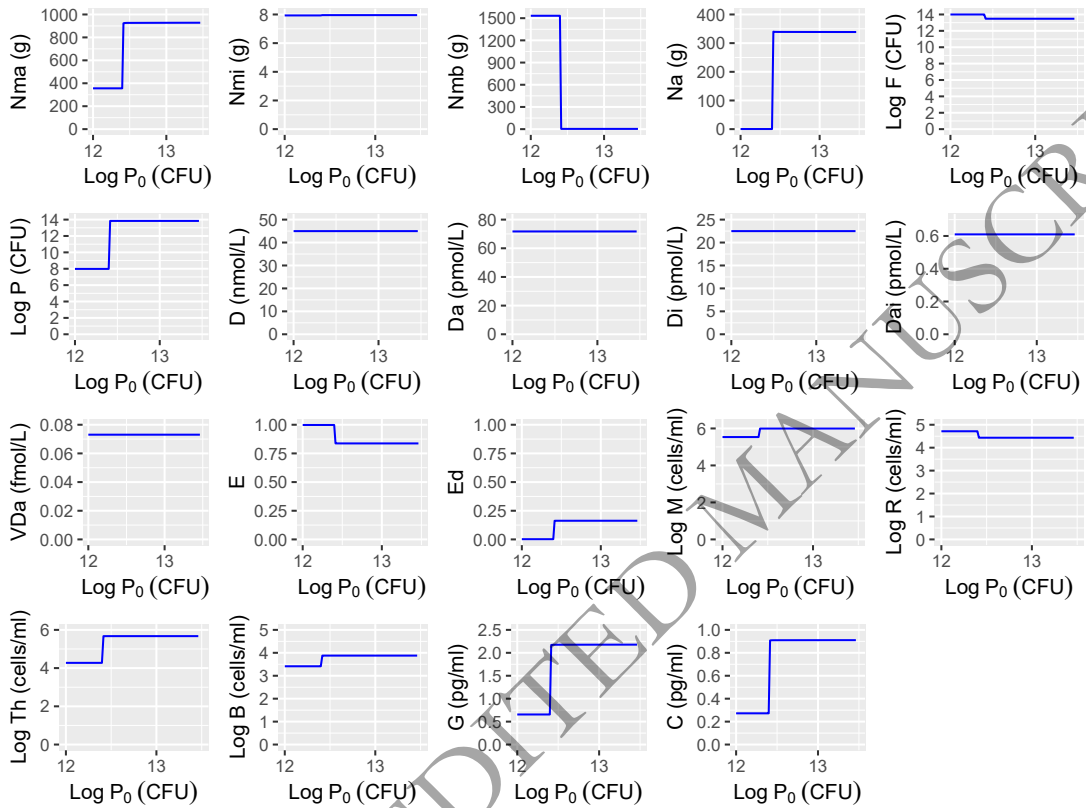


FIG. 14. The predicted steady state concentrations of nutrients, bacterial populations, epithelial cells and immune response from solving equations (2.1)-(2.26) with baseline parameters given in Tables 2-5 with increasing initial pathogen population  $P_0$  and decreasing commensal population  $F_0$ . Initial conditions are given by equations (2.7), (2.16) and (2.26) with  $P_0$  increasing from  $1 \times 10^{12}$  to  $0.5 \times 10^{14}$  and  $F_0$  remaining constant at  $0.5 \times 10^{14}$ . Probiotic and vitamin D supplementation is not considered.

473 is caused by an imbalance in bacterial composition and simulate this by changing the initial composition  
 474 of commensal and pathogenic bacteria based on the steady state solutions predicted for the inflammatory  
 475 case in Figure 6. Initial conditions for the remaining variables do not change. A comparison between  
 476 the predicted values of the model variables for the two scenarios is presented in Figures 15-17.

477 Model predictions are similar to those obtained for the individual sub-models with the population  
 478 of pathogenic bacteria growing under inflammatory conditions, heightening the immune response and  
 479 causing damage to the host epithelial cells. Pro-inflammatory compounds enhance the production of  
 480 alternative nutrients (in Figure 15,  $N_a$  at steady state increases from 0.4g to 340g between the non-  
 481 inflammatory and inflammatory states) which are utilised by the pathogenic bacteria so that they  
 482 dominate over the commensals. Enhanced production of alternative nutrients is often seen with severe  
 483 inflammation and may reflect a dysregulated/inappropriate immune response as observed in cytokine  
 484 storms and sepsis. It is worth noting however, that the upregulated immune response doesn't appear to  
 485 suppress the pathogen population.

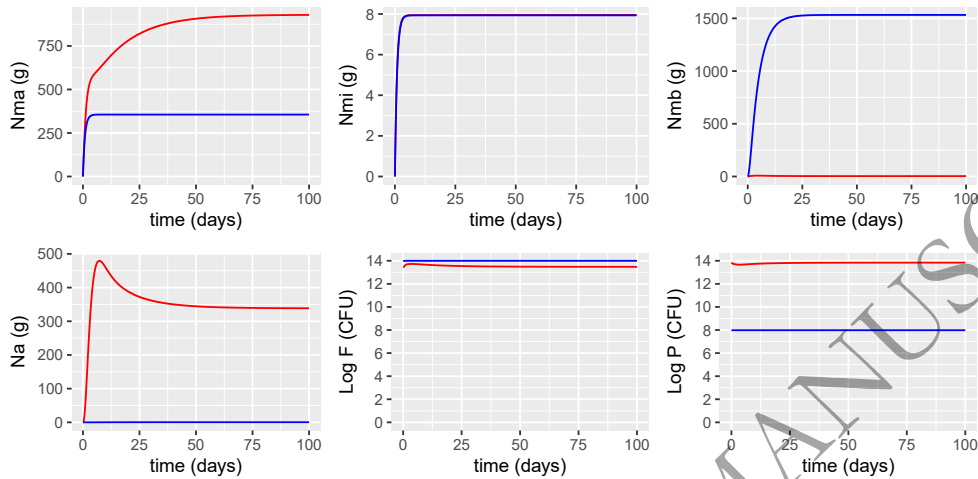


FIG. 15. The predicted concentrations of macronutrients, micronutrients, metabolites, alternate nutrients and populations of commensal and pathogenic bacteria, from solving equations (2.1)-(2.26) with baseline parameters given in Tables 2-5 for an individual with normobiosis (blue) and dysbiosis (red). Initial conditions are given by equations (2.7), (2.16) and (2.26) but in the dysbiosis case, the initial populations of commensal and pathogenic bacteria are altered so that  $F_0 = 2.86 \times 10^{13}$  and  $P_0 = 7.07 \times 10^{13}$  at  $t = 0$ . These values have been taken from the inflammatory case in Figure 6. Probiotic and vitamin D supplementation is not considered.

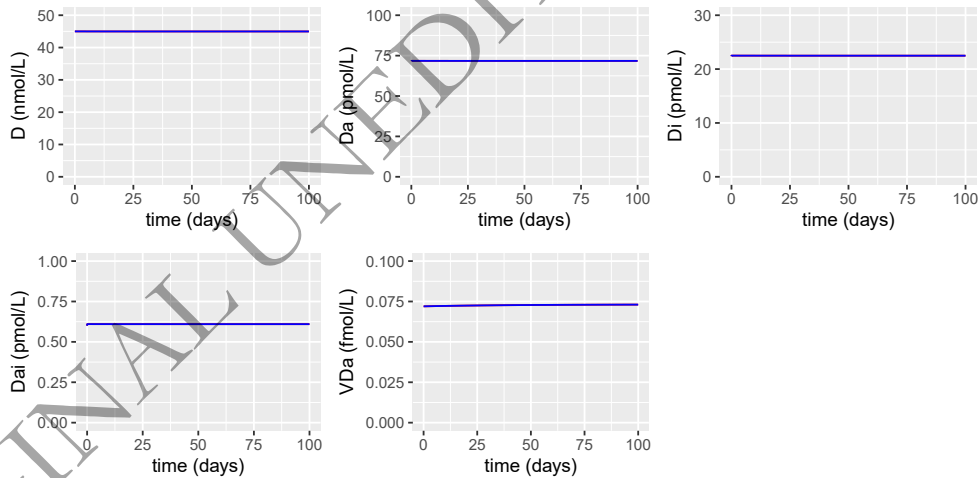


FIG. 16. The predicted time evolution of extracellular and intracellular 25(OH)D and 1,25(OH)<sub>2</sub>D and the VDR:1,25(OH)<sub>2</sub>D complex, from solving equations (2.1)-(2.26) with baseline parameters given in Tables 2-5 for an individual with normobiosis (blue) and dysbiosis (red). Initial conditions are given by equations (2.7), (2.16) and (2.26) but in the dysbiosis case, the initial populations of commensal and pathogenic bacteria are altered so that  $F_0 = 2.86 \times 10^{13}$  and  $P_0 = 7.07 \times 10^{13}$  at  $t = 0$ . These values have been taken from the inflammatory case in Figure 6. Probiotic and vitamin D supplementation is not considered.



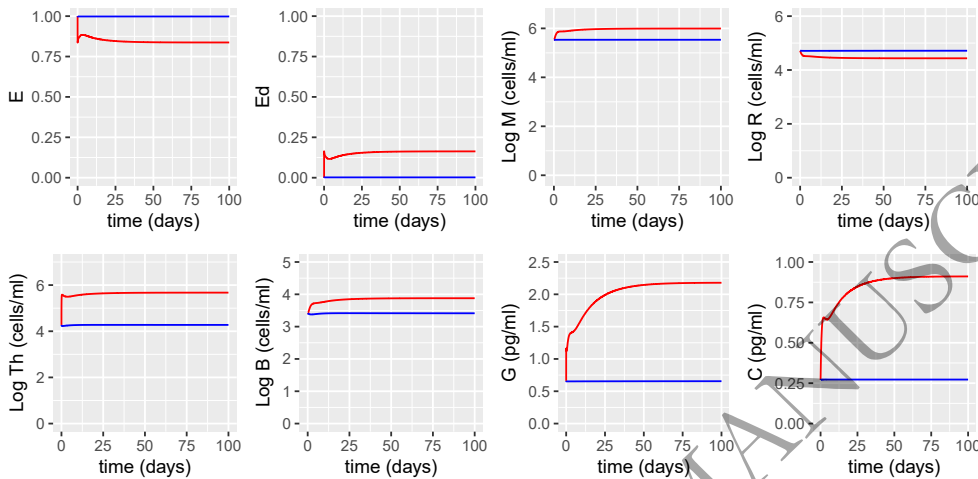


FIG. 17. The predicted volume fraction of healthy and damaged epithelial cells, densities of macrophages, regulatory cells, Th cells and plasma B cells and concentrations of anti- and pro-inflammatory cytokines, from solving equations (2.1)-(2.26) with baseline parameters given in Tables 2-5 for an individual with normobiosis (blue) and dysbiosis (red). Initial conditions are given by equations (2.7), (2.16) and (2.26) but in the dysbiosis case, the initial populations of commensal and pathogenic bacteria are altered so that  $F_0 = 2.86 \times 10^{13}$  and  $P_0 = 7.07 \times 10^{13}$  at  $t = 0$ . These values have been taken from the inflammatory case in Figure 6. Probiotic and vitamin D supplementation is not considered.

### 3.2. Vitamin D supplementation

Approximately 50% of the global population have insufficient levels of vitamin D (50-75 nmol/L) and around 35% are deficient (<50 nmol/L) (Nair et al. 2012, Palacios et al. 2014). We therefore explore the impact of vitamin D supplementation on individuals with various initial serum 25(OH)D concentrations. Simulation of the same dose of vitamin D ( $D^0$ ) being given to both vitamin D deficient and sufficient (>75 nmol/L) individuals on the resulting serum levels of 25(OH)D is shown in Figure 18.

All individuals eventually attain the same steady state concentration of serum 25(OH)D following supplementation, but the most deficient individuals take longer to achieve this concentration. Supplementation therefore has less of an effect on healthy individuals and the simulation suggests that those that are deficient need to take supplements for longer to have the greatest benefit.

We now examine the effect of changing the dose of vitamin D,  $D^0$ , on a deficient individual with levels of inflammation predicted in Figures 15-17 for dysbiosis. Simulations of the serum levels of 25(OH)D and its metabolites with supplementation corresponding to 10-20  $\mu\text{g}/\text{day}$ , no supplementation and a reduced vitamin D intake are presented in Figure 19.

The serum levels of 25(OH)D increase approximately linearly with vitamin D intake, reaching a maximum steady state concentration following a constant daily dose at around 80 days. When intake of vitamin D is too low, levels of 25(OH)D decrease, so that the individual becomes vitamin D deficient. Doses of 10, 15 and 20  $\mu\text{g}/\text{day}$  all result in concentrations of 25(OH)D above the healthy serum level (75 nmol/L) thought to be necessary to maximise the effect of vitamin D on calcium, bone and muscle metabolism (Holick et al. 2011, Rosen et al. 2012) and compare favourably with the profile of measured serum vitamin D levels in healthy older adults supplemented with varying doses of vitamin D over six months presented in Figure 2A in Graeff-Adams et al. 2020.

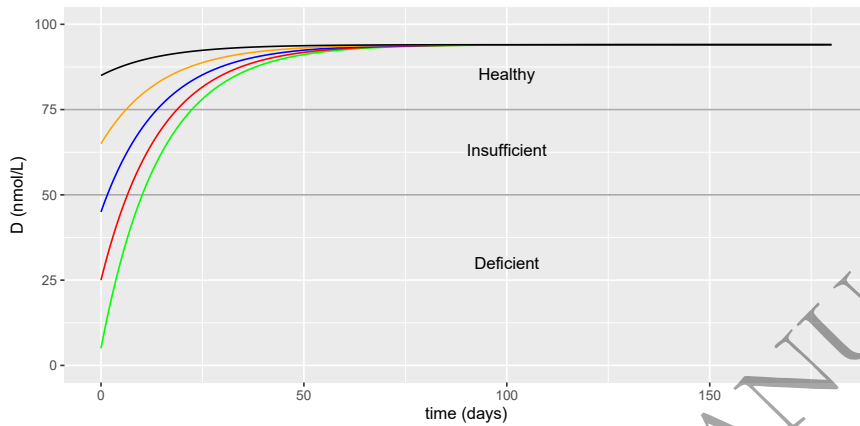


FIG. 18. Simulations predicting the effect of vitamin D supplementation on individuals with varying initial serum concentrations of 25(OH)D solving equations (2.1)-(2.25) with baseline parameters given in Tables 2-5. The initial serum concentrations of 25(OH)D are  $D_0 = 5$  (green), 25 (red), 45 (blue), 65 (orange), and 85 (black) nmol/L and the intake rate  $D^0 = 5$  nmol/L day<sup>-1</sup>.

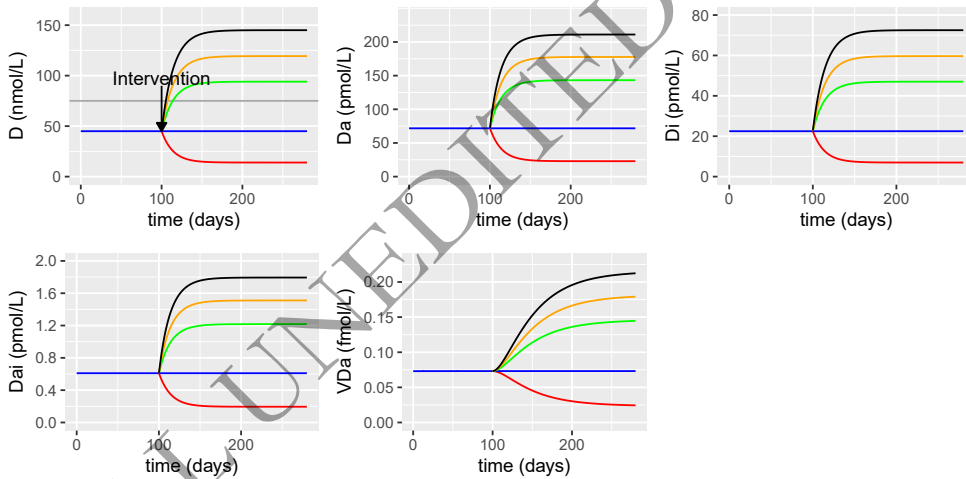


FIG. 19. The predicted time evolution of extracellular and intracellular 25(OH)D and 1,25(OH)<sub>2</sub>D and the VDR:1,25(OH)<sub>2</sub>D complex with increasing vitamin D intake from solving equations (2.1)-(2.25) with baseline parameters given in Tables 2-5. Initial conditions are assumed to be the steady state values predicted in Figures 15-17 for the dysbiosis case. A daily intervention of vitamin D supplements is administered from day 100. Simulations represent reduced intake of vitamin D ( $D^0 = 1$  nmol/L day<sup>-1</sup>) (red), no supplementation ( $D^0 = 3.2$  nmol/L day<sup>-1</sup>) (blue), supplementation of 10  $\mu$ g/day of 25(OH)D ( $D^0 = 6.5$  nmol/L day<sup>-1</sup>) (green), 15  $\mu$ g/day ( $D^0 = 8.3$  nmol/L day<sup>-1</sup>) (orange) and 20  $\mu$ g/day ( $D^0 = 10$  nmol/L day<sup>-1</sup>) (black).

508 Increasing vitamin D intake also increases extracellular 1,25(OH)<sub>2</sub>D, intracellular 25(OH)D,  
 509 intracellular 1,25(OH)<sub>2</sub>D and the VDR:1,25(OH)<sub>2</sub>D complex. While we observe a linear relationship  
 510 between 25(OH)D and 1,25(OH)<sub>2</sub>D, experimentally Tang et al. 2019 did not observe a strong  
 511 correlation in their serum concentrations despite a direct enzymatic conversion between them. However,  
 512 as shown in Chun et al. 2012, Beetjes et al. 2019 and Tang et al. 2019, there is an upward trend of

513 serum levels of  $1,25(\text{OH})_2\text{D}$  with increasing serum  $25(\text{OH})\text{D}$  and our predictions are within the range  
 514 observed. The serum and intracellular concentrations of  $25(\text{OH})\text{D}$  and  $1,25(\text{OH})_2\text{D}$  reach a maximum  
 515 steady state concentration at approximately the same duration after supplementation commences i.e. at  
 516 80 days, but the  $\text{VDR}:1,25(\text{OH})_2\text{D}$  complex does not attain steady state until much later, at around 180  
 517 days.

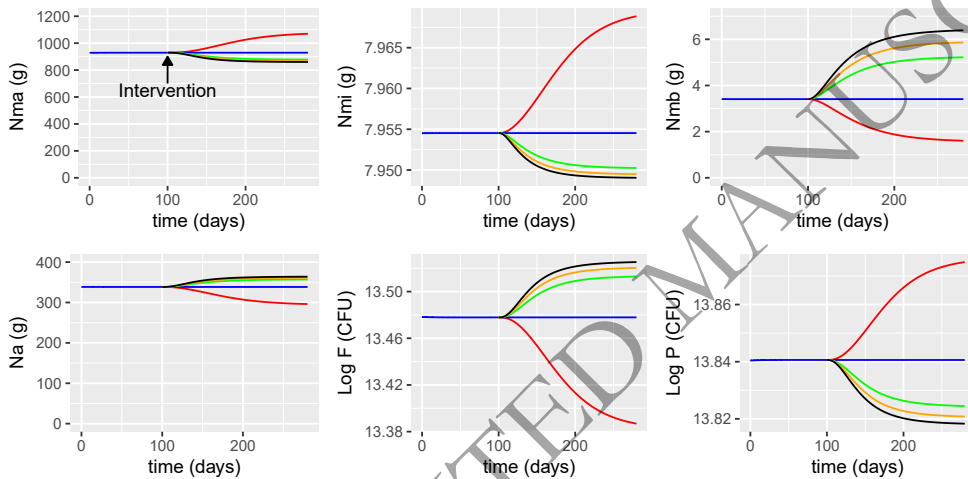


FIG. 20. The predicted concentrations of macronutrients, micronutrients, metabolites, alternate nutrients and populations of commensal and pathogenic bacteria with increasing vitamin D intake from solving equations (2.1)-(2.25) with baseline parameters given in Tables 2-5. Initial conditions are assumed to be the steady state values predicted in Figures 15-17 for the dysbiosis case. A daily intervention of vitamin D supplements is administered from day 100. Simulations represent reduced intake of vitamin D ( $D^0 = 1 \text{ nmol/L day}^{-1}$ ) (red), no supplementation ( $D^0 = 3.2 \text{ nmol/L day}^{-1}$ ) (blue), supplementation of  $10 \mu\text{g/day}$  of  $25(\text{OH})\text{D}$  ( $D^0 = 6.5 \text{ nmol/L day}^{-1}$ ) (green),  $15 \mu\text{g/day}$  ( $D^0 = 8.3 \text{ nmol/L day}^{-1}$ ) (orange) and  $20 \mu\text{g/day}$  ( $D^0 = 10 \text{ nmol/L day}^{-1}$ ) (black). Note the magnified scale of the vertical axes for  $N_{mi}$ ,  $\text{Log } F$  and  $\text{Log } P$  in order to observe more clearly the effect of supplementation on these variables.

518 Figures 20 and 21 show the nutrient concentrations, bacterial populations, epithelial cells and  
 519 immune response with increasing vitamin D intake. With no intervention, vitamin D concentrations  
 520 remain constant and epithelial cells under low-level stress release pro-inflammatory cytokines that  
 521 stimulate macrophages, plasma B cells and Th cells. When the vitamin D intake is reduced, the vitamin  
 522 D receptor complex is downregulated, decreasing the density of regulatory cells and increasing the  
 523 production of pro-inflammatory cytokines by the damaged epithelial cells and hence the densities of  
 524 macrophages, Th cells and plasma B cells. Anti-inflammatory mediators also increase, dampening down  
 525 the effect of the inflammatory cytokines. There is small decrease in the concentration of metabolites as  
 526 more are converted into alternate nutrients by pathogen-induced inflammation.

527 When vitamin D intake increases, the  $\text{VDR}$  complex is upregulated, which helps repair the  
 528 epithelial barrier. An increase in  $\text{VDR}$  also promotes the development of regulatory cells, inhibits  
 529 T cell proliferation and pro- and anti-inflammatory cytokine production, impairs the activation of  
 530 macrophages and B cells and increases the population of commensal bacteria and concentration of  
 531 metabolites.

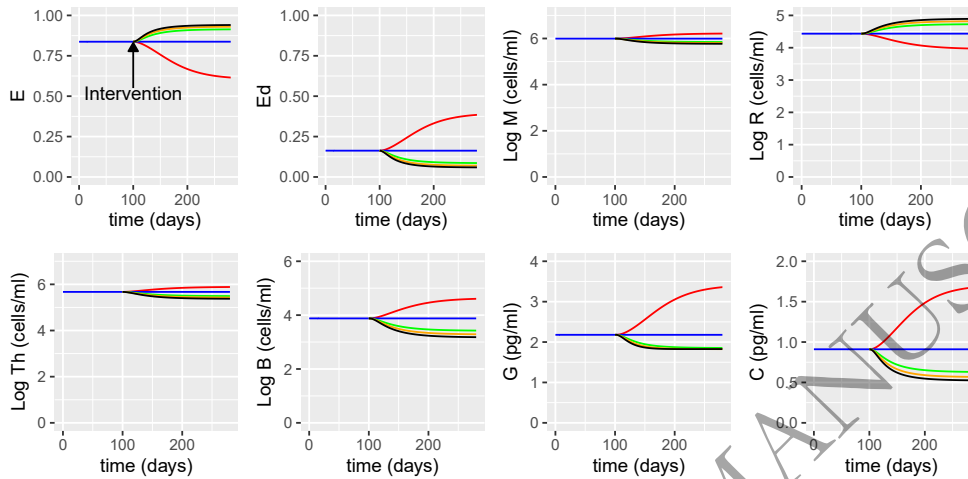


FIG. 21. The predicted volume fraction of healthy and damaged epithelial cells, densities of macrophages, regulatory cells, Th cells and plasma B cells and concentrations of anti- and pro-inflammatory cytokines with increasing vitamin D intake from solving equations (2.1)-(2.25) with baseline parameters given in Tables 2-5. Initial conditions are assumed to be the steady state values predicted in Figures 15-17 for the dysbiosis case. A daily intervention of vitamin D supplements is administered from day 100. Simulations represent reduced intake of vitamin D ( $D^0 = 1 \text{ nmol/L day}^{-1}$ ) (red), no supplementation ( $D^0 = 3.2 \text{ nmol/L day}^{-1}$ ) (blue), supplementation of  $10 \mu\text{g/day}$  of 25(OH)D ( $D^0 = 6.5 \text{ nmol/L day}^{-1}$ ) (green),  $15 \mu\text{g/day}$  ( $D^0 = 8.3 \text{ nmol/L day}^{-1}$ ) (orange) and  $20 \mu\text{g/day}$  ( $D^0 = 10 \text{ nmol/L day}^{-1}$ ) (black).

532 Figure 22 shows a summary of the predicted populations of commensal and pathogenic  
 533 bacteria, concentration of VDR:1,25(OH)<sub>2</sub>D complex, volume fraction of healthy epithelial cells and  
 534 concentration of pro-inflammatory cytokines following the constant daily intervention of vitamin D  
 535 supplements (intakes ranging from 1-10 nmol/L day<sup>-1</sup>) for 180 days presented in Figures 19-21. The  
 536 concentration of  $V_{D_a}$  increases linearly with vitamin D intake but  $F$ ,  $P$ ,  $E$  and  $C$  all saturate with high  
 537 doses, indicating that there is a diminishing return on health benefit for higher doses of vitamin D intake.

### 538 3.3. Probiotic supplementation

539 The effect of daily administration of probiotics on the model variables is shown in Figures 23-25.  
 540 Increasing doses of probiotics ( $P_b$ ) ranging from no supplements to  $2 \times 10^{10}$  CFU/day were given from  
 541 day 100 without vitamin D supplementation.

542 Following supplementation, the serum concentration of 25(OH)D and its metabolites increase but  
 543 this is not a linear effect. Similarly, the increase in healthy epithelial cells and decrease in immune  
 544 cell density is not linear with probiotic intake. In agreement with Jones et al. 2013, serum vitamin D  
 545 increased by approximately 25% after probiotic administration. As for vitamin D supplementation, the  
 546 upregulation of the VDR:1,25(OH)<sub>2</sub>D complex in response to probiotics dampens down inflammation  
 547 and increases the volume fraction of healthy epithelial and regulatory cells but to a lesser extent than  
 548 that observed in Figure 21.

549 Figure 26 shows a summary of the predicted populations of commensal and pathogenic  
 550 bacteria, concentration of VDR:1,25(OH)<sub>2</sub>D complex, volume fraction of healthy epithelial cells and  
 551 concentration of pro-inflammatory cytokines following the constant daily intervention of probiotic  
 552 supplements (intakes ranging from 100-1×10<sup>11</sup> CFU/day) for 180 days presented in Figures 23-25.

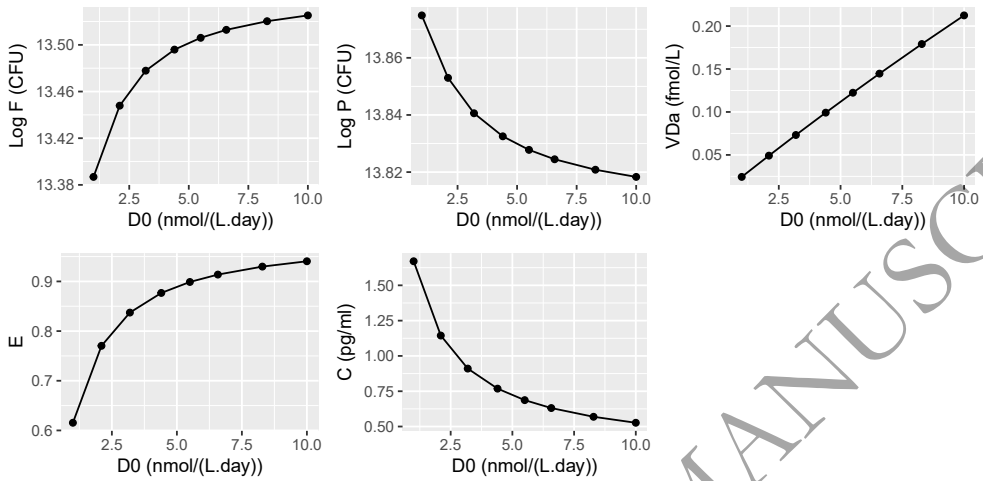


FIG. 22. The predicted populations of commensal and pathogenic bacteria, concentration of VDR:1,25(OH)<sub>2</sub>D complex, volume fraction of healthy epithelial cells and concentration of pro-inflammatory cytokines on day 180 following daily intervention of vitamin D supplements from day 0 determined from solving equations (2.1)-(2.25) with baseline parameters given in Tables 2-5. Vitamin D intake ranges from  $D^0 = 1 - 10 \text{ nmol/L day}^{-1}$  and initial conditions are assumed to be the steady state values predicted in Figures 15-17 for the dysbiosis case.

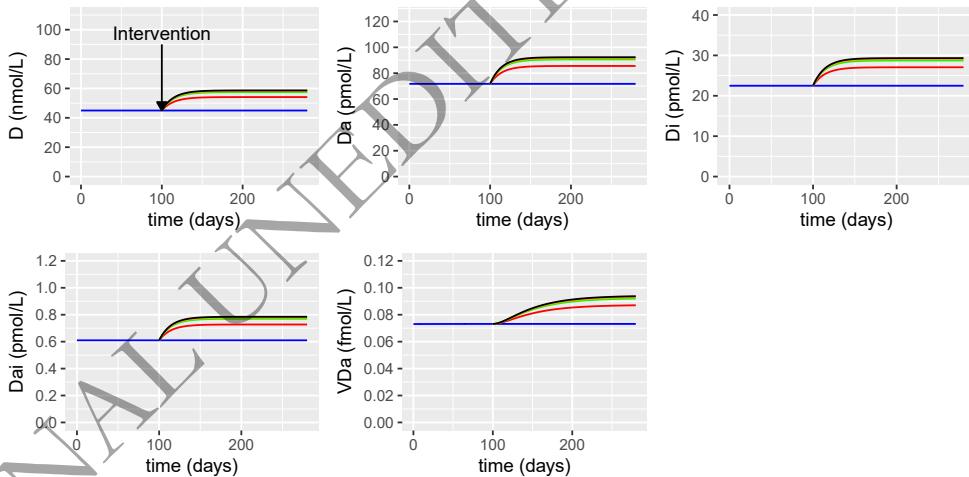


FIG. 23. The predicted concentrations of extracellular and intracellular 25(OH)D and 1,25(OH)<sub>2</sub>D and VDR:1,25(OH)<sub>2</sub>D complex with increasing probiotic intake from solving equations (2.1)-(2.25) with baseline parameters given in Tables 2-5. Initial conditions are assumed to be the steady state values predicted in Figures 15-17 for the dysbiosis case. A daily intervention of probiotic supplements is administered from day 100. Simulations represent no supplements ( $P_b = 0$ ) (blue),  $P_b = 1 \times 10^9 \text{ CFU/day}$  (red),  $5 \times 10^9 \text{ CFU/day}$  (green),  $1 \times 10^{10} \text{ CFU/day}$  (orange),  $1 \times 10^{11} \text{ CFU/day}$  (black).

553 All variables remain unchanged until the intake of probiotics exceeds approximately  $1 \times 10^7 \text{ CFU/day}$   
 554 when  $F$ ,  $V_{D_a}$  and  $E$  start to increase and  $P$  and  $C$  decrease.  $E$ ,  $C$  and  $V_{D_a}$  all saturate with high doses  
 555 indicating that there is a diminishing improvement in epithelial barrier repair and anti-inflammatory

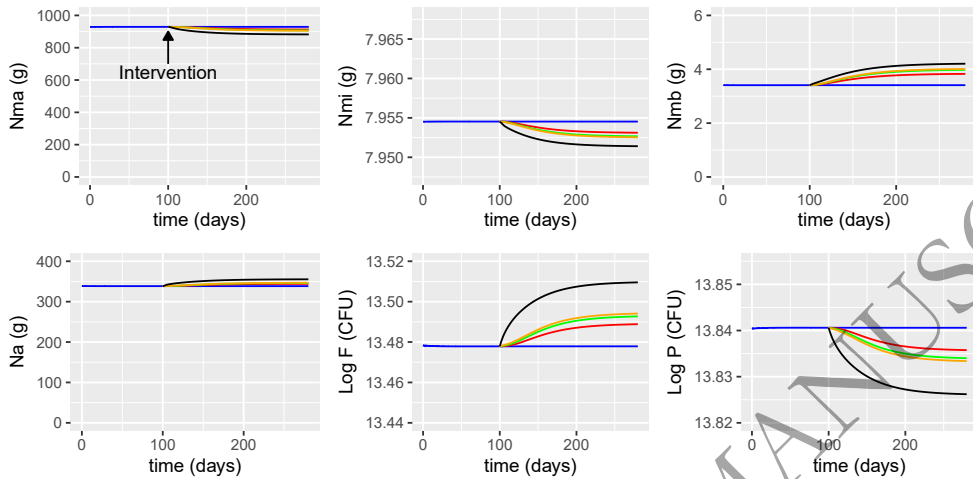


FIG. 24. The predicted concentrations of macronutrients, micronutrients, metabolites, alternate nutrients and populations of commensal and pathogenic bacteria with increasing probiotic intake from solving equations (2.1)-(2.25) with baseline parameters given in Tables 2-5. Initial conditions are assumed to be the steady state values predicted in Figures 15-17 for the dysbiosis case. A daily intervention of probiotic supplements is administered from day 100. Simulations represent no supplements ( $P_b = 0$ ) (blue),  $P_b = 1 \times 10^9$  CFU/day (red),  $5 \times 10^9$  CFU/day (green),  $1 \times 10^{10}$  CFU/day (orange),  $1 \times 10^{11}$  CFU/day (black). Note the magnified scale of the vertical axes for  $N_{mi}$ ,  $\text{Log } F$  and  $\text{Log } P$  in order to observe more clearly the effect of supplementation on these variables.

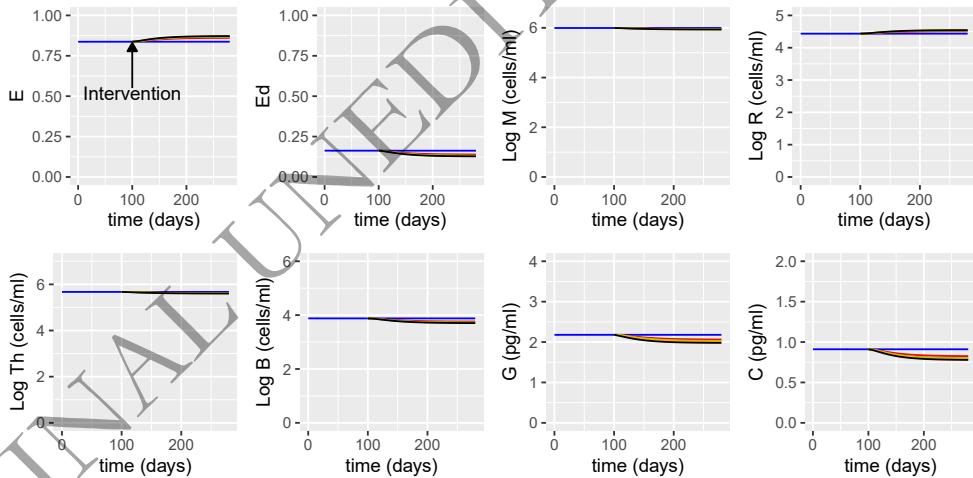


FIG. 25. The predicted volume fraction of healthy and damaged epithelial cells, densities of macrophages, regulatory cells, Th cells and plasma B cells and concentrations of anti- and pro-inflammatory cytokines with increasing probiotic intake from solving equations (2.1)-(2.25) with baseline parameters given in Tables 2-5. Initial conditions are assumed to be the steady state values predicted in Figures 15-17 for the dysbiosis case. A daily intervention of probiotic supplements is administered from day 100. Simulations represent no supplements ( $P_b = 0$ ) (blue),  $P_b = 1 \times 10^9$  CFU/day (red),  $5 \times 10^9$  CFU/day (green),  $1 \times 10^{10}$  CFU/day (orange),  $1 \times 10^{11}$  CFU/day (black).

556 benefits for higher doses of probiotic intake. However, the bacterial populations continue to increase  
 557 (commensals) and decrease (pathogens) at high doses.

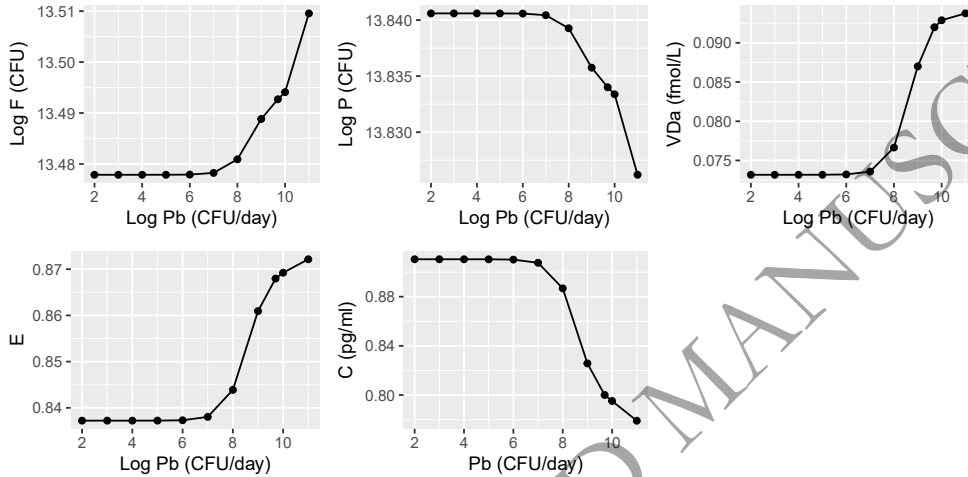


FIG. 26. The predicted populations of commensal and pathogenic bacteria, concentration of VDR:1,25(OH)<sub>2</sub>D complex, volume fraction of healthy epithelial cells and concentration of pro-inflammatory cytokines on day 180 following daily intervention of probiotic supplements from day 0 determined from solving equations (2.1)-(2.25) with baseline parameters given in Tables 2-5. Probiotic intake ranges from  $P_b = 100 - 1 \times 10^{11}$  CFU/day and initial conditions are assumed to be the steady state values predicted in Figures 15-17 for the dysbiosis case.

### 558 3.4. Vitamin D and probiotic supplementation

559 Simulations predicting the effect of combining vitamin D and probiotic supplements and comparing  
 560 levels with those predicted with no supplements, vitamin D only and probiotics only are shown in  
 561 Figures 27-29. Daily supplements are administered individually or in combination on day 100 and the  
 562 response of the nutrient concentrations, bacteria populations, levels of vitamin D and its metabolites,  
 563 volume fraction of epithelial cells and the immune response before and after the intervention are  
 564 predicted numerically.

565 As with the individual supplementation described in the previous two subsections, administration  
 566 of vitamin D and/or probiotic supplements upregulates the vitamin D receptor which helps repair the  
 567 epithelial barrier function and stimulates the production of regulatory cells. An increase in macrophages  
 568 enhances the capacity for VDR:1,25(OH)<sub>2</sub>D-mediated elimination of pathogenic bacteria, resulting in  
 569 an upregulation of commensal bacteria and metabolites as more SCFAs are being produced, providing  
 570 energy for epithelial cell proliferation. Concomitantly, the same VDR:1,25(OH)<sub>2</sub>D interaction is able  
 571 to modify antigen-presentation and activated T cell function to promote attenuation of inflammatory  
 572 T cell responses and enhance tolerogenic regulatory cell activity. In this way vitamin D can act as a  
 573 double-edged sword within the immune system by enhancing innate antimicrobial immunity, whilst  
 574 simultaneously protecting against potential tissue damage associated with over-exuberant adaptive  
 575 immunity.

576 As observed in the individual models, vitamin D supplements enhance the positive effects more than  
 577 probiotics but taking them in combination results in the greatest benefit. However, co-supplementation



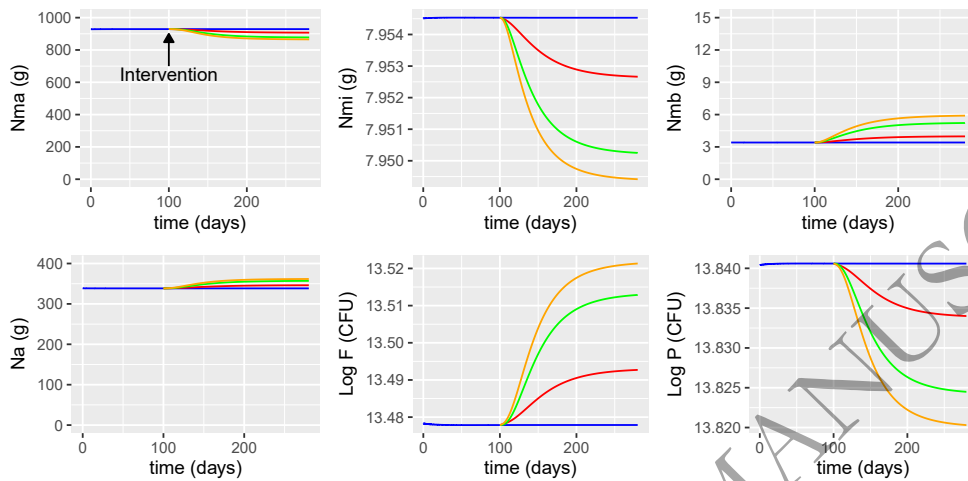


FIG. 27. The predicted concentrations of macronutrients, micronutrients, metabolites, alternate nutrients and populations of commensal and pathogenic bacteria with vitamin D and probiotic co-supplementation from solving equations (2.1)-(2.25) with baseline parameters given in Tables 2-5. Initial conditions are assumed to be the steady state values predicted in Figures 15-17 for the dysbiosis case. A daily intervention is administered from day 100. Simulations represent no supplements ( $P_b = 0$ ,  $D^0 = 3.2$  nmol/L day $^{-1}$ ) (blue), probiotic supplement only ( $P_b = 5 \times 10^9$  CFU/day,  $D^0 = 3.2$  nmol/L day $^{-1}$ ) (red), vitamin D supplement only ( $P_b = 0$ ,  $D^0 = 6.5$  nmol/L day $^{-1}$ ) (green) and combined vitamin D and probiotic supplements ( $P_b = 5 \times 10^9$  CFU/day,  $D^0 = 6.5$  nmol/L day $^{-1}$ ) (orange). Note the magnified scale of the vertical axes for  $N_{mi}$ , Log  $F$  and Log  $P$  in order to observe more clearly the effect of supplementation on these variables.

578 produces a combined effect that is less than the sum of the two separate supplements administered  
 579 individually. This is illustrated more clearly in Figure 30, where a comparison between the steady states  
 580 of the metrics  $F$ ,  $P$ ,  $D$ ,  $V_{D_a}$ ,  $E$  and  $C$  for the different supplementation regimens is shown.

#### 581 4. Discussion

582 Clinical studies examining the possible interactions between vitamin D/VDR pathway and probiotic  
 583 administration in modulating intestinal inflammation are emerging, and results from initial studies  
 584 provide a promising therapeutic option for a variety of human diseases (Abboud et al. 2020, Pagnini  
 585 et al. 2021). The principal aim of this study was to develop a novel mathematical model to describe  
 586 the possible interactions between probiotics and vitamin D for promoting intestinal homeostasis and  
 587 immune health.

588 Mechanistic information and clinical observations from the literature were used to develop the  
 589 model and inform parameter values where possible. The model simulates the concentration of nutrients  
 590 in the intestine, populations of commensal and pathogenic bacteria, the concentrations of vitamin D and  
 591 its metabolites, the volume fractions of healthy and damaged epithelial cells, the densities of immune  
 592 cells and the concentrations of anti- and pro-inflammatory mediators with and without supplementation.  
 593 However, the model is sensitive to the choice of parameters and the lack of information on certain  
 594 parameters, particularly in the immune response model, is a limitation of this study. A better  
 595 understanding of the parameters that govern the bacterial and inflammatory response is essential for  
 596 more quantitative predictions.

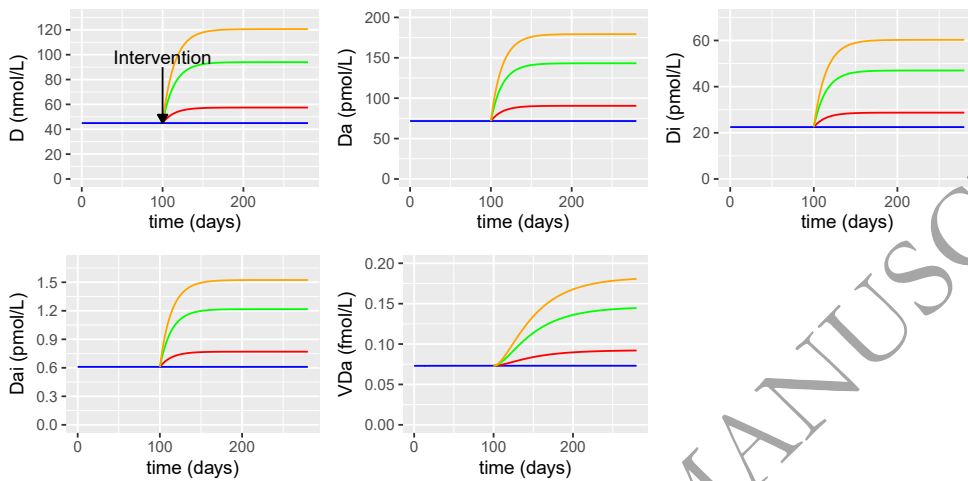


FIG. 28. The predicted concentrations of extracellular and intracellular 25(OH)D and 1,25(OH)<sub>2</sub>D and VDR:1,25(OH)<sub>2</sub>D complex with vitamin D and probiotic co-supplementation from solving equations (2.1)-(2.25) with baseline parameters given in Tables 2-5. Initial conditions are assumed to be the steady state values predicted in Figures 15-17 for the dysbiosis case. A daily intervention is administered from day 100. Simulations represent no supplements ( $P_b = 0$ ,  $D^0 = 3.2$  nmol/L day<sup>-1</sup>) (blue), probiotic supplement only ( $P_b = 5 \times 10^9$  CFU/day,  $D^0 = 3.2$  nmol/L day<sup>-1</sup>) (red), vitamin D supplement only ( $P_b = 0$ ,  $D^0 = 6.5$  nmol/L day<sup>-1</sup>) (green) and combined vitamin D and probiotic supplements ( $P_b = 5 \times 10^9$  CFU/day,  $D^0 = 6.5$  nmol/L day<sup>-1</sup>) (orange).

Nevertheless, the parameters have been chosen so that the model is able to predict similar qualitative behaviour to that observed clinically and our attempt to understand the mechanistic interactions between the intestinal microbiota, immune response and vitamin D and probiotic supplementation has highlighted the need for future experimental studies measuring, for example, the microbiota composition, immune cell phenotypes, inflammatory markers, dietary intake, intestinal barrier integrity markers and markers of vitamin D homeostasis.

Vitamin D levels are low in the UK population (Hyppönen et al. 2007), and in most other populations, and vitamin D levels among British adults are inversely associated with infection risk (Berry et al. 2011), suggesting that the influence of low vitamin D status on immune competence is a public health problem. Our model has been able to illustrate the potential benefits of supplementation and indicates how the administration of vitamin D supplements to deficient individuals could help them attain the desired vitamin D levels, while suggesting that supplementation has less of an effect on healthy individuals. The model has also predicted that vitamin D supplementation upregulates the VDR complex, which enhances barrier function (and hence increases AMP production by epithelial cells), maintains innate and cell-mediated immunity and prevents low-grade inflammation. In Ogbu et al. 2020, it is hypothesised that an upregulation of VDR may increase the commensal production of SFCAs and this proposed behaviour has been captured in our model.

Specific strains of probiotics have different functions and mechanisms of action. They need to survive the passage through the upper gastrointestinal tract and colonise the intestine so that they can affect the immune system positively. By incorporating probiotic supplementation into the input terms in the equations representing the commensal bacteria population and serum concentration of 25(OH)D, our model has suggested that administration of probiotics supports the maintenance of

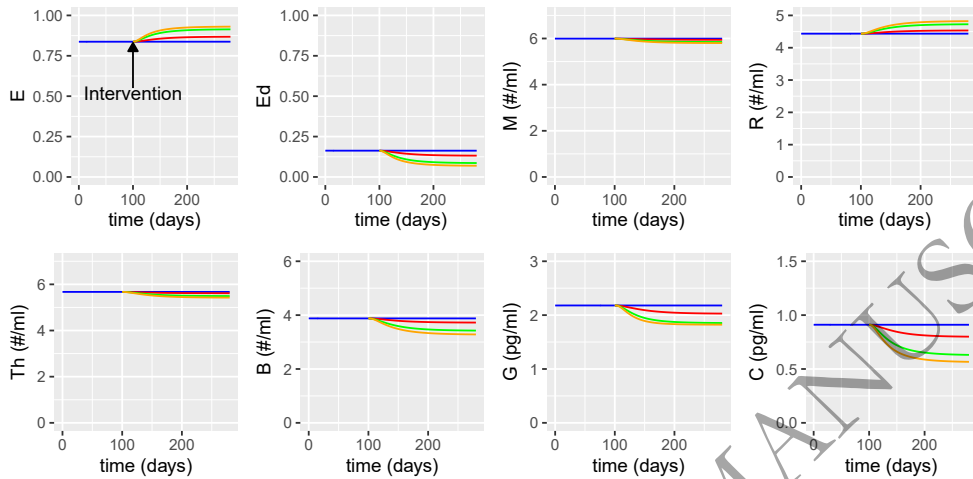


FIG. 29. The predicted volume fractions of healthy and damaged epithelial cells, densities of macrophages, regulatory cells, Th cells and plasma B cells and concentrations of anti- and pro-inflammatory cytokines with vitamin D and probiotic co-supplementation from solving equations (2.1)-(2.25) with baseline parameters given in Tables 2-5. Initial conditions are assumed to be the steady state values predicted in Figures 15-17 for the dysbiosis case. A daily intervention is administered from day 100. Simulations represent no supplements ( $P_b = 0$ ,  $D^0 = 3.2 \text{ nmol/L day}^{-1}$ ) (blue), probiotic supplement only ( $P_b = 5 \times 10^9 \text{ CFU/day}$ ,  $D^0 = 3.2 \text{ nmol/L day}^{-1}$ ) (red), vitamin D supplement only ( $P_b = 0$ ,  $D^0 = 6.5 \text{ nmol/L day}^{-1}$ ) (green) and combined vitamin D and probiotic supplements ( $P_b = 5 \times 10^9 \text{ CFU/day}$ ,  $D^0 = 6.5 \text{ nmol/L day}^{-1}$ ) (orange).

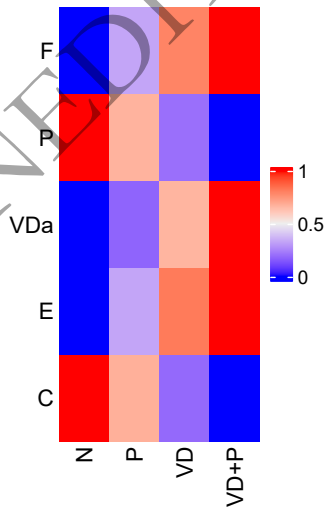


FIG. 30. A comparison summary of the normalised populations of commensal and pathogenic bacteria, concentration of VDR:1.25(OH)<sub>2</sub>D complex, volume fraction of healthy epithelial cells and concentration of pro-inflammatory cytokines predicted on day 180 following no supplementation (N) and daily interventions of probiotics only (P), vitamin D only (VD) and vitamin D and probiotic co-supplementation (VD+P) from day 0 taken from Figures 27-29.

619 immune cells, enhances intestinal barrier function and protects against intestinal inflammation by  
620 mediating inflammatory signalling molecules. The model has also predicted that co-supplementation  
621 of vitamin D and probiotics increases the positive effects, as vitamin D intestinal absorption and VDR  
622 protein expression are upregulated, enhancing their anti-inflammatory benefits. Whilst there are benefits  
623 of combining the two supplements the overall effect is less than the sum of the individual ones and  
624 unfortunately, the model does not predict the same synergistic effects of co-supplementation intimated  
625 in some studies reviewed by [Abboud et al. 2020](#). This indicates that more clinical studies and a greater  
626 understanding of the parameters needs to be carried out to clarify the health benefits.

627 Under inflammatory conditions our model has predicted the loss of intestinal barrier function and  
628 growth of the pathogenic bacteria. This can result in the translocation of pathogenic bacteria and their  
629 structural components into the bloodstream causing inflammation elsewhere in the body. The structural  
630 complexity and functional capability of the intestinal microbiota declines with poor diet and age and  
631 is likely a factor causing immunosenescence in older people ([Wu et al. 2021](#)). Extending our model to  
632 examine these spatial aspects is an interesting area for future study.

633 The relationship between the intestinal microbiota and human health is an area of increasing interest,  
634 and our model, which is parameterised as fully as the available literature allows, is the first to explore  
635 the complex interactions between the various mechanistic components and determine the impact of  
636 manipulating the intestinal microbiota with dietary components. Despite our many assumptions, the  
637 model produces biologically realistic predictions and hence would seem to provide a credible basis for  
638 future work in this area.

### 639 **Acknowledgements**

640 This work was supported by a UKRI Nutrition Research Partnership Award (grant number  
641 MR/T001879/1). JRK gratefully acknowledges a Royal Society Leverhulme Trust Senior Fellowship.

### 642 **Appendix A**

643 Sensitivity of the full model to local changes in the baseline parameters given in Tables 2-5 is shown  
644 in Figures 31 (microbiota model parameters), 32 (vitamin D model parameters) and 33 (epithelial and  
645 immune response model parameters) for variables  $F$ ,  $P$ ,  $V_{D_a}$ ,  $E$  and  $C$ .

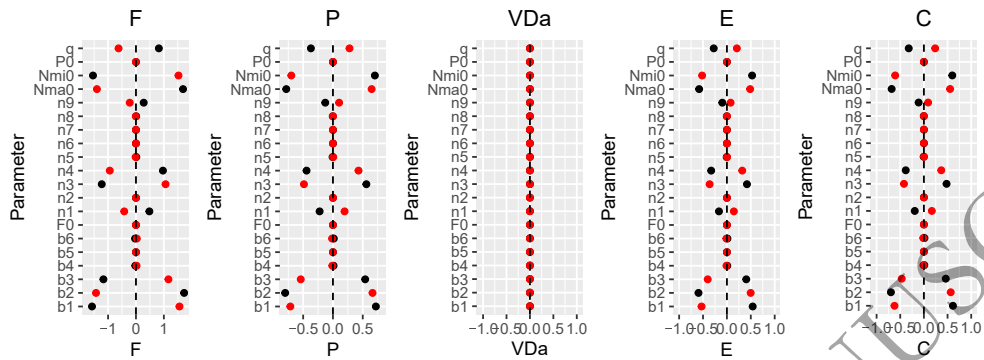


FIG. 31. The effect of varying parameter values on the steady state bacteria populations, VDR:1,25(OH)<sub>2</sub>D complex, volume fraction of healthy epithelial cells and concentration of pro-inflammatory cytokines. Baseline parameter values are taken from Tables 2 and each parameter is sequentially varied by a 10% decrease (black) and a 10% increase (red). Sensitivity is defined by equation (2.8). Note that  $n=\eta$  and  $b=\beta$ .

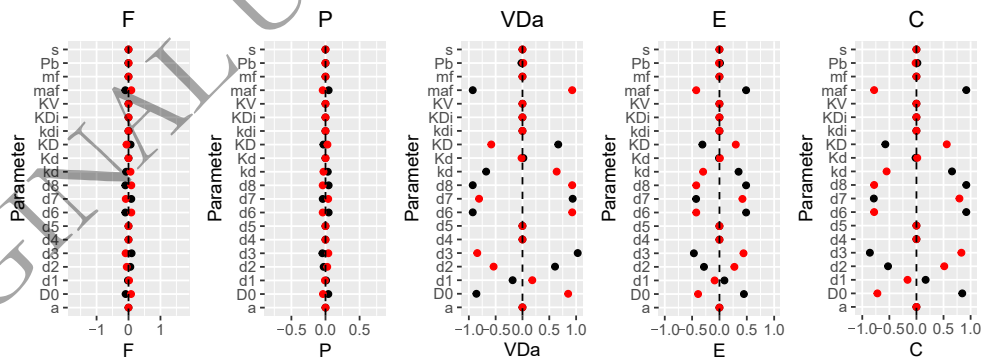


FIG. 32. The effect of varying parameter values on the steady state bacteria populations, VDR:1,25(OH)<sub>2</sub>D complex, volume fraction of healthy epithelial cells and concentration of pro-inflammatory cytokines. Baseline parameter values are taken from Tables 3 and each parameter is sequentially varied by a 10% decrease (black) and a 10% increase (red). Sensitivity is defined by equation (2.8). Note that  $m=\mu$ ,  $d=\delta$ .

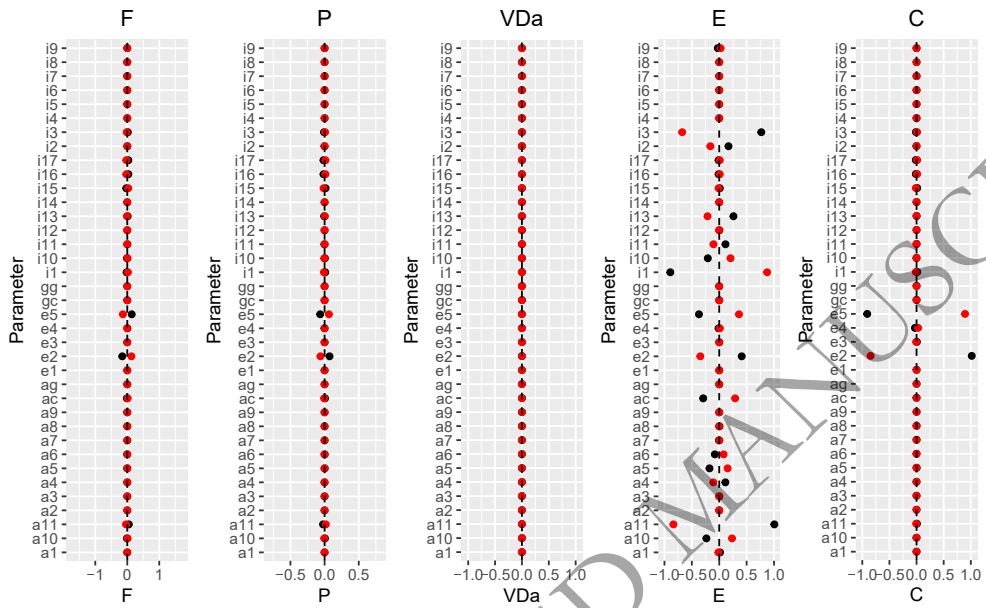


FIG. 33. The effect of varying parameter values on the steady state bacteria populations, VDR:1,25(OH)<sub>2</sub>D complex, volume fraction of healthy epithelial cells and concentration of pro-inflammatory cytokines. Baseline parameter values are taken from Tables 4 and 5 and each parameter is sequentially varied by a 10% decrease (black) and a 10% increase (red). Sensitivity is defined by equation (2.8). Note that  $i=t$ ,  $a=\alpha$ ,  $e=\epsilon$  and  $g=\gamma$ .

## REFERENCES

646

647 1. Abboud, M., Rizk, R., AlAnouti, F., Papandreou, D., Haidar, S. & Mahboub, N. (2020) The Health Effects  
648 of Vitamin D and Probiotic Co-Supplementation: A Systematic Review of Randomized Controlled Trials.  
649 *Nutrients*, Dec 30;13(1):111. doi: 10.3390/nu13010111.

650 2. Adrian, M. (2020) Understanding the human gut microbiome: A mathematical approach.  
651 *Undergraduate thesis. University of Iowa.*, [https://iro.uiowa.edu/discovery/delivery/01IOWA\\_INST:](https://iro.uiowa.edu/discovery/delivery/01IOWA_INST:ResearchRepository/12811139520002771?#13811408760002771)  
652 [ResearchRepository/12811139520002771?#13811408760002771](https://iro.uiowa.edu/discovery/delivery/01IOWA_INST:ResearchRepository/12811139520002771?#13811408760002771).

653 3. Bakke, D., Chatterjee, I., Agrawal, A., Dai, Y. & Sun, J. (2018) Regulation of Microbiota by  
654 Vitamin D Receptor: A Nuclear Weapon in Metabolic Diseases. *Nucl. Receptor Res.*, 5:101377. doi:  
655 10.11131/2018/101377.

656 4. Beentjes, C.H.L., Taylor-King, J.P., Bayani, A., Davis, C.N., Dunster, J.L., Jabbari, S., Mirams, G.R.,  
657 Jenkinson, C., Kilby, M.D., Hewison, M. & Tamblyn, J.A. (2019) Defining vitamin D status using multi-  
658 metabolite mathematical modelling: A pregnancy perspective. *J. Steroid Biochem. Mol. Biol.*, Jun;190:152-160.  
659 doi: 10.1016/j.jsbmb.2019.03.024.

660 5. Berry, D.J., Hesketh, K., Power, C. & Hyppönen, E. (2011) Vitamin D status has a linear association  
661 with seasonal infections and lung function in British adults. *Br. J. Nutr.*, Nov;106(9):1433-40. doi:  
662 10.1017/S0007114511001991.

663 6. Bishop, E., Ismailova, A., Dimeloe, S., Hewison, M. & White, J.H. (2020) Vitamin D and Immune Regulation:  
664 Antibacterial, Antiviral, Anti-Inflammatory. *JBMR Plus.*, Sep 15;5(1):e10405. doi: 10.1002/jbm4.10405.

665 7. Chun, R.F., Peercy, B.E., Adams, J.S. & Hewison, M. (2012) Vitamin D binding protein and monocyte  
666 response to 25-hydroxyvitamin D and 1,25-dihydroxyvitamin D: analysis by mathematical modeling. *PLoS*  
667 *One.*, 7(1):e30773. doi: 10.1371/journal.pone.0030773.

668 8. Conlon, M.A. & Bird, A.R. (2014) The impact of diet and lifestyle on gut microbiota and human health.  
669 *Nutrients.*, Dec 24;7(1):17-44. doi: 10.3390/nu7010017.

670 9. Cristofori, F., Dargenio, V.N., Dargenio, C., Miniello, V.L., Barone, M. & Francavilla, R. (2021) Anti-  
671 Inflammatory and Immunomodulatory Effects of Probiotics in Gut Inflammation: A Door to the Body. *Front*  
672 *Immunol.*, Feb 26;12:578386. doi: 10.3389/fimmu.2021.578386.

673 10. De Maeyer, R.P.H. & Chambers, E.S. The impact of ageing on monocytes and macrophages. *Immunol. Lett.*,  
674 Feb;230:1-10. doi: 10.1016/j.imlet.2020.12.003.

675 11. de Vos, P., Mujagic, Z., de Haan, B.J., Siezen, R.J., Bron, P.A., Meijerink, M., Wells, J.M., Masclee, A.A.M.,  
676 Boekschoten, M.V., Faas, M.M. & Troost, F.J. (2017) Lactobacillus plantarum Strains Can Enhance Human  
677 Mucosal and Systemic Immunity and Prevent Non-steroidal Anti-inflammatory Drug Induced Reduction in T  
678 Regulatory Cells. *Front Immunol.*, Aug 23;8:1000. doi: 10.3389/fimmu.2017.01000.

679 12. Fan, Y. & Pedersen, O. (2021) Gut microbiota in human metabolic health and disease. *Nat. Rev. Microbiol.*,  
680 Jan;19(1):55-71. doi: 10.1038/s41579-020-0433-9.

681 13. Graeff-Armas, L.A., Bendik, I., Kunz, I., Schoop, R., Hull, S. & Beck, M. (2020) Supplemental  
682 25-Hydroxycholecalciferol Is More Effective than Cholecalciferol in Raising Serum 25-Hydroxyvitamin D  
683 Concentrations in Older Adults. *J. Nutr.*, Jan 1;150(1):73-81. doi: 10.1093/jn/nxz209.

684 14. Hara, A. & Iwasa, Y. (2019) Coupled dynamics of intestinal microbiome and immune system-A mathematical  
685 study. *J. Theor. Biol.*, Mar 7;464:9-20. doi: 10.1016/j.jtbi.2018.12.021.

686 15. Holick, M.F., Binkley, N.C., Bischoff-Ferrari, H.A., Gordon, C.M., Hanley, D.A., Heaney, R.P., Murad, M.H.  
687 & Weaver, C. (2011) Evaluation, treatment, and prevention of vitamin D deficiency: an Endocrine Society  
688 Clinical Practice Guideline. *J. Clin. Endocrinol. Metab.*, 96:1911-30.

689 16. Hyppönen, E. & Power, C. (2007) Hypovitaminosis D in British adults at age 45 y: nationwide cohort study  
690 of dietary and lifestyle predictors. *Am. J. Clin. Nutr.*, 85:860-868. doi: 10.1093/ajcn/85.3.860.

691 17. Jones, M.L., Martoni, C.J. & Prakash, S. (2013) Oral supplementation with probiotic *L. reuteri* NCIMB 30242  
692 increases mean circulating 25-hydroxyvitamin D: a post hoc analysis of a randomized controlled trial. *J. Clin.*  
693 *Endocrinol. Metab.*, Jul;98(7):2944-51. doi: 10.1210/jc.2012-4262.



- 694 18. Karmali, R., Hewison, M., Rayment, N., Farrow, S.M., Brennan, A., Katz, D.R., O’Riordan, J.L. (1991)  
695 1,25(OH)<sub>2</sub>D<sub>3</sub> regulates c-myc mRNA levels in tonsillar T lymphocytes. *Immunology*, Dec;74(4):589-93.
- 696 19. Kumar, M., Ji, B., Zengler, K. & Nielsen, J. (2019) Modelling approaches for studying the microbiome. *Nat.*  
697 *Microbiol.*, Aug;4(8):1253-1267. doi: 10.1038/s41564-019-0491-9.
- 698 20. Lang, J.M., Eisen, J.A. & Zivkovic, A.M. (2014) The microbes we eat: abundance and taxonomy of microbes  
699 consumed in a day’s worth of meals for three diet types. *PeerJ*, Dec 9;2:e659. doi: 10.7717/peerj.659.
- 700 21. Lopez, D.V., Al-Jaberi, F.A.H., Woetmann, A., Ødum, N., Bonefeld, C.M., Kongsbak-Wismann, M., Geisler,  
701 C. (2021) Macrophages Control the Bioavailability of Vitamin D and Vitamin D-Regulated T Cell Responses.  
702 *Front. Immunol.*, Sep 21;12:722806. doi: 10.3389/fimmu.2021.722806.
- 703 22. Lu, R., Shang, M., Zhang, Y.G., Jiao, Y., Xia, Y., Garrett, S., Bakke, D., Bäuerl, C., Martinez, G.P.,  
704 Kim, C.H., Kang, S.M. & Sun, J. (2020) Lactic Acid Bacteria Isolated From Korean Kimchi Activate  
705 the Vitamin D Receptor-autophagy Signaling Pathways. *Inflamm. Bowel Dis.*, Jul 17;26(8):1199-1211. doi:  
706 10.1093/ibd/izaa049.
- 707 23. Magnúsdóttir, S. & Thiele, I. (2018) Modeling metabolism of the human gut microbiome. *Curr. Opin.*  
708 *Biotechnol.*, Jun;51:90-96. doi: 10.1016/j.copbio.2017.12.005.
- 709 24. Mujagic, Z., de Vos, P., Boekschoten, M.V., Govers, C., Pieters, H.H., de Wit, N.J., Bron, P.A., Masclee,  
710 A.A. & Troost, F.J. (2017) The effects of *Lactobacillus plantarum* on small intestinal barrier function and  
711 mucosal gene transcription; a randomized double-blind placebo controlled trial. *Sci Rep.*, Jan 3;7:40128. doi:  
712 10.1038/srep40128.
- 713 25. Nair, R. & Maseeh, A. (2012) Vitamin D: The “sunshine” vitamin. *J. Pharmacol. Pharmacother.*,  
714 Apr;3(2):118-26. doi: 10.4103/0976-500X.95506.
- 715 26. Nielsen, O.H, Rejnmark, L., Moss & A.C. (2018) Role of Vitamin D in the Natural History of Inflammatory  
716 Bowel Disease. *J. Crohns Colitis*, May 25;12(6):742-752. doi: 10.1093/ecco-jcc/jjy025.
- 717 27. Ogbu, D., Xia, E. & Sun, J. (2020) Gut instincts: vitamin D/vitamin D receptor and microbiome in  
718 neurodevelopment disorders. *Open Biol.*, Jul;10(7):200063. doi: 10.1098/rsob.200063.
- 719 28. Pagnini, C., Di Paolo, M.C., Graziani, M.G. & Delle Fave, G. (2021) Probiotics and Vitamin D/Vitamin  
720 D Receptor Pathway Interaction: Potential Therapeutic Implications in Inflammatory Bowel Disease. *Front*  
721 *Pharmacol.*, Nov 24;12:747856. doi: 10.3389/fphar.2021.747856.
- 722 29. Palacios, C. & Gonzalez, L. (2014) Is vitamin D deficiency a major global public health problem? *J. Steroid*  
723 *Biochem. Mol. Biol.*, Oct;144 Pt A:138-45. doi: 10.1016/j.jsbmb.2013.11.003.
- 724 30. Pickard, J.M., Zeng, M.Y., Caruso, R. & Núñez, G. (2017) Gut microbiota: Role in pathogen colonization,  
725 immune responses, and inflammatory disease. *Immunol. Rev.*, Sep;279(1):70-89. doi: 10.1111/immr.12567.
- 726 31. Rosen, C.J., Abrams, S.A., Aloia, J.F., Brannon, P.M., Clinton, S.K., Durazo-Arvizu, R.A., Gallagher JC,  
727 Gallo, R.L., Jones, G., Kovacs, C.S., Manson, J.E., Mayne, S.T., Ross, A.C., Shapses, S.A. & Taylor, C.L.  
728 (2012) IOM committee members respond to Endocrine Society vitamin D guidelines. *J. Clin. Endocrinol.*  
729 *Metab.*, 97:1146-52.
- 730 32. Salazar, N., Arboleya, S., Fernández-Navarro, T., de Los Reyes-Gavilán, C.G., Gonzalez, S. & Gueimonde, M.  
731 (2019) Age-Associated Changes in Gut Microbiota and Dietary Components Related with the Immune System  
732 in Adulthood and Old Age: A Cross-Sectional Study. *Nutrients.*, Jul 31;11(8):1765. doi: 10.3390/nu11081765.
- 733 33. Sender, R., Fuchs, S. & Milo, R. (2016) Are We Really Vastly Outnumbered? Revisiting the Ratio of Bacterial  
734 to Host Cells in Humans. *Cell.*, Jan 28;164(3):337-40. doi: 10.1016/j.cell.2016.01.013.
- 735 34. Shashkova, T., Popenko, A., Tyakht, A., Peskov, K., Kosinsky, Y., Bogolubsky, L., Raigorodskii, A., Ischenko,  
736 D., Alexeev, D. & Govorun, V. (2016) Agent Based Modeling of Human Gut Microbiome Interactions and  
737 Perturbations. *PLoS One.*, Feb 19;11(2):e0148386. doi: 10.1371/journal.pone.0148386.
- 738 35. Singh, P., Rawat, A., Alwakeel, M., Sharif, E. & Al Khodor, S. (2020) The potential role of  
739 vitamin D supplementation as a gut microbiota modifier in healthy individuals. *Sci. Rep.*, 10,21641.  
740 <https://doi.org/10.1038/s41598-020-77806-4>.
- 741 36. Smith, P.D., Smythies, L.E., Shen, R., Greenwell-Wild, T., Gliozzi, M. & Wahl, S.M. (2011) Intestinal  
742 macrophages and response to microbial encroachment. *Mucosal Immunol.*, 4(1):31-42. doi: 10.1038/mi.2010.66.

- 743 37. Souberbielle, J.C., Massart, C., Brailly-Tabard, S., Cavalier, E. & Chanson, P. (2016) Prevalence  
744 and determinants of vitamin D deficiency in healthy French adults: the VARIETE study. *Endocrine.*,  
745 Aug;53(2):543-50. doi: 10.1007/s12020-016-0960-3.
- 746 38. Stojanov, S., Berlec, A. & Štrukelj, B. (2020) The Influence of Probiotics on the Firmicutes/Bacteroidetes  
747 Ratio in the Treatment of Obesity and Inflammatory Bowel disease. *Microorganisms.*, Nov 1;8(11):1715. doi:  
748 10.3390/microorganisms8111715.
- 749 39. Stübler, S., Kloft, C. & Huisinga, W. (2023) Cell-level systems biology model to study inflammatory  
750 bowel diseases and their treatment options. *CPT Pharmacometrics Syst. Pharmacol.*, May;12(5):690-705. doi:  
751 10.1002/psp4.12932.
- 752 40. Tang, J.C.Y., Jackson, S., Walsh, N.P., Greeves, J. & Fraser, W.D.; Bioanalytical Facility team. (2019) The  
753 dynamic relationships between the active and catabolic vitamin D metabolites, their ratios, and associations with  
754 PTH. *Sci. Rep.*, May 6;9(1):6974. doi: 10.1038/s41598-019-43462-6.
- 755 41. Tangestani, H., Boroujeni, H.K., Djafarian, K., Emamat, H. & Shab-Bidar, S. (2021) Vitamin D  
756 and The Gut Microbiota: a Narrative Literature Review. *Clin Nutr Res.*, Jul 20;10(3):181-191. doi:  
757 10.7762/cnr.2021.10.3.181.
- 758 42. Wu, Y.L., Xu, J., Rong, X.Y., Wang, F., Wang, H.J. & Zhao, C. (2021) Gut microbiota alterations and  
759 health status in aging adults: From correlation to causation. *Aging Med. (Milton)*, Jun 24;4(3):206-213. doi:  
760 10.1002/agm2.12167.
- 761 43. Xong, X., Fu, J., Xu, B., Wang, Y. & Jin, M. (2020) Interplay between gut microbiota and antimicrobial  
762 peptides. *Anim Nutr.*, Dec;6(4):389-396. doi: 10.1016/j.aninu.2020.09.002.
- 763 44. Yamamoto, E.A. & Jørgensen, T.N. (2020) Relationships Between Vitamin D, Gut Microbiome, and Systemic  
764 Autoimmunity. *Front. Immunol.*, Jan 21;10:3141. doi: 10.3389/fimmu.2019.03141.
- 765 45. Zheng, D., Liwinski, T. & Elinav, E. (2020) Interaction between microbiota and immunity in health and  
766 disease. *Cell Res.*, Jun;30(6):492-506. doi: 10.1038/s41422-020-0332-7.
- 767 46. Zhou, A., Yuan, Y., Yang, M., Huang, Y., Li, X., Li, S., Yang, S. & Tang, B. (2022) Crosstalk Between the Gut  
768 Microbiota and Epithelial Cells Under Physiological and Infectious Conditions. *Front. Cell. Infect. Microbiol.*,  
769 Jan 27;12:832672. doi: 10.3389/fcimb.2022.832672.